



Review

Covid-19 imaging: A narrative review

Hanae Ramdani^{*}, Nazik Allali, Latifa Chat, Siham El Haddad

Radiology Department, Childrens' Hospital - Ibn Sina University Hospital-Rabat, Lamfadel Cherkaoui Street, 10010, Rabat, Morocco

ARTICLE INFO

Keywords:

COVID-19

Sars-Cov2

Novel coronavirus

Imaging

Computed tomography (CT)

Chest

ABSTRACT

Background: The 2019 novel coronavirus disease (COVID-19) imaging data is dispersed in numerous publications. A cohesive literature review is to be assembled.

Objective: To summarize the existing literature on Covid-19 pneumonia imaging including precautionary measures for radiology departments, Chest CT's role in diagnosis and management, imaging findings of Covid-19 patients including children and pregnant women, artificial intelligence applications and practical recommendations.

Methods: A systematic literature search of PubMed/med line electronic databases.

Results: The radiology department's staff is on the front line of the novel coronavirus outbreak. Strict adherence to precautionary measures is the main defense against infection's spread. Although nucleic acid testing is Covid-19's pneumonia diagnosis gold standard; kits shortage and low sensitivity led to the implementation of the highly sensitive chest computed tomography amidst initial diagnostic tools. Initial Covid-19 CT features comprise bilateral, peripheral or posterior, multilobar ground-glass opacities, predominantly in the lower lobes. Consolidations superimposed on ground-glass opacifications are found in few cases, preponderantly in the elderly. In later disease stages, GGO transformation into multifocal consolidations, thickened interlobular and intralobular lines, crazy paving, traction bronchiectasis, pleural thickening, and subpleural bands are reported. Standardized CT reporting is recommended to guide radiologists. While lung ultrasound, pulmonary MRI, and PET CT are not Covid-19 pneumonia's first-line investigative diagnostic modalities, their characteristic findings and clinical value are outlined. Artificial intelligence's role in strengthening available imaging tools is discussed.

Conclusion: This review offers an exhaustive analysis of the current literature on imaging role and findings in COVID-19 pneumonia.

1. Introduction

The emerging Covid-19 pandemic continues its rapid spread challenging healthcare systems worldwide in a new and unpredictable manner. Communication and shared experience are key elements to better understand the infection and thus control it through rapid diagnosis, early quarantine and prompt treatment [1]. In the face of the extremely communicable SARS-COV2 outbreak, continual assessment of the highly-dynamic available data, further large systematic analyses and prospective observational and clinical trials are essential to protect communities and healthcare personnel, prepare human capital, arrange infrastructure, effectively manage patients and surveil public health [2, 3]. Alongside with epidemiological history, clinical characteristics and laboratory findings; imaging plays an invaluable role in early recognition, triage, prognosis prediction and may be of use in therapeutic

evaluation and follow-up of Covid-19 pneumonia [4–6]. This report summarizes precautionary measures for radiology departments whose staff is on the front line of this alarming outbreak, Chest CT's role in diagnosis and management, imaging findings of COVID-19 patients including children and pregnant women, artificial intelligence applications in this setting and practical recommendations.

2. Radiology department organization

Radiology departments' strict adherence to robust protective protocols is mandatory to minimize virus spread via droplets transmission and contaminated equipment [7,8]. Non urgent exams are rescheduled while hospitalized and urgent external patients' studies (malignancies in particular) are performed [9,10]. On-site staff is reduced, rotations are established and the largest possible number of functionaries work from

^{*} Corresponding author.

E-mail addresses: hanaeramdani@hotmail.fr (H. Ramdani), n_allali@yahoo.fr (N. Allali), chatlatifa@hotmail.com (L. Chat), sihamelhaddad@gmail.com (S. El Haddad).

<https://doi.org/10.1016/j.amsu.2021.102489>

Received 20 April 2021; Received in revised form 31 May 2021; Accepted 5 June 2021

Available online 18 June 2021

2049-0801/© 2021 The Authors. Published by Elsevier Ltd on behalf of IJS Publishing Group Ltd. This is an open access article under the CC BY license

(<http://creativecommons.org/licenses/by/4.0/>).

home. Deployment in high-priority areas is a possibility to prepare for [9,10]. Training programs are suspended [10]. Social distancing is implemented. Videoconferencing and telephone are utilized whenever practicable [9,10]. Employees are taught how to appropriately use Personal protective equipment (PPE) with emphasis on the necessity of regular and thorough washing of hands [9]. Wearing a mask (surgical or rather a respirator), eye protection (goggles or face shield), an isolation disposable gown and gloves is recommended when in close contact with suspected or confirmed Covid-19 patients. Shoe covers and a surgical cap could be added [7–9]. When possible, portable imaging limits suspected patients' movement [8]. If transportation to the radiology unit is needed, patients are to take a well-delineated path and wear a surgical mask throughout transfer and examination [7,9]. Dedicated CT scanners reduce contamination and allow high throughput as the needed exam (unenhanced chest CT) is rapidly performed [11,12]. Reserving consecutive time periods on a designated scanner for suspected or confirmed covid-19 cases is another practical option to manage workflow and reduce cleansing's ensuing down-time [7,12]. Alone in the CT room, the radiographer performs the exam. Images are then transferred to the radiologist for interpretation [9,12]. Each contact with a high-risk patient is to be followed by CT gantry and all possibly contaminated surfaces disinfection using vendor's suggested detergent solutions [7].

3. Chest computed tomography

3.1. Chest CT's role in diagnosis and management

Confirmatory diagnosis of Covid-19 infection relies on the real-time reverse transcription-polymerase chain reaction (RT-PCR) nucleotides detection from respiratory tract samples [13]; a method with several shortcomings: High specificity but limited sensitivity (60–70%) generating false negative results [14,15], especially at early disease phases [16]. These false negatives may be due to an insufficient viral load in specimens-the lower respiratory tract samples being the most sensitive [17]-, inadequate extraction techniques, sampling timing [18], differences in RT-PCR tests sensitivity and laboratory errors [15,19–21]. They require reiterated assays that burden potentially insufficient infrastructure, overload the testing kits supply and impede quarantine measures with the possibility of unchecked contaminations [22,23]. Biological samples analysis is time-consuming [9]. The consequent delay in results obtainment obstructs the timely needed decisions of maintained isolated medical surveillance or discharge of suspected patients under investigation [11,18]. Chest CT complements viral nucleic acid detection with a considerable sensitivity reaching 97% in epidemic territories [14]. Rapid, simple to carry out and available, it may show typical Covid-19 imaging features preceding RT-PCR tests positivity in the initial disease stages [24]. In this setting, isolation measures are undertaken as quickly as possible to prevent additional infection spread [19]. Moreover, CT examination shows both disease evolution and gravity while RT-PCR only makes a positive diagnosis [19].

3.2. COVID-19 pneumonia's chest CT features

3.2.1. Imaging findings

Initial Covid-19 CT features comprise bilateral, peripheral or posterior, multilobar ground-glass opacities, predominantly in the lower lobes and less commonly within the middle lobe. Consolidations superimposed on ground-glass opacifications are found in few cases, preponderantly in the elderly. In later disease stages, GGO transformation into multifocal consolidations, thickened interlobular and intralobular lines, crazy paving, traction bronchiectasis, pleural thickening, and subpleural bands are reported. Pleural/pericardial effusion, enlarged mediastinal lymphadenopathies, cavities, CT halo sign, and pneumothorax are infrequent but can be observed with pneumonia's evolution [4].

Dai et al. evaluated 234 covid-19 patients' high-resolution chest CTs.

15 (6,4%) exams showed no abnormalities. Abnormal attenuations in several bilateral lung lobes were described in 192 cases (87.67% 192/219). Anomalies concerned the entire lung in 121 patients (63.02%, 121/192), and only 16 patients (7.3%, 16/219) presented an isolated lobe lesion. Lesions were located in the lower lungs and/or lung periphery in 208 cases (94.98%, 208/219), and appeared in an irregular (88.3%, 193/219), little patches (86.3%, 189/219), bands-like (69.41%, 152/219), circular (49.32%, 108/219) and 'anti-butterfly' fashion (47.95%, 105/219). 60 patients (27.4%, 60/219) had an underlying pulmonary disease; emphysema most frequently (88.33%, 53/60), succeeded by bronchiectasia (16.67%, 10/60). Other reported signs included in order of frequency: vascular enhancement sign, interlobular septal thickening, air bronchogram, bronchiectasis, pleural thickening, solid nodules, reticular sign, fissures shift and bronchial walls thickening. 29 patients presented slight pleural and pericardial effusions. In 21 cases, mediastinal lymphadenopathy was depicted [21] (Fig. 1).

Li et al. retrospectively analyzed chest CT images of 131 confirmed Covid-19 patients from 3 chinese hospital establishments. 6 initial CT scans were normal whilst the remaining 125 examinations revealed bilateral lung participation in 104 cases (79%). In 100 cases (76%); lesions' distribution was peripheral. 115 patients (87%) showed multiple abnormalities (>3). 106 patients (81%) presented patchy ground glass opacities, 91 patients (69%) had patchy consolidations and 40 patients (31%) exhibited nodules. 10 patients displayed diffuse, bilateral pulmonary involvement with 'white lungs' appearance. Interlobular septal thickening was described in 68 cases (52%) and crazy paving in 8 cases. Vascular enhancement sign, air bronchograms and fibrosis signs were also reported. Unusual findings were: isolated nodules in 7 cases only, reversed halo sign, pleural thickening, pleural/pericardial effusions and mediastinal lymphadenopathy. 1 case of consolidation with a cavity was reported, and represented an exceptional finding [25].

In Guan et al.' study, two chest radiologists individually examined fifty-three thin-section chest CTs of confirmed COVID-19 patients. 47 patients (88.7%) presented Covid-19 pneumonia findings whilst 6 scans were normal (11.3%). Total cases showed ground glass opacities, among which 59.6% were circular and 40.4% patchy. 89.4% of cases presented crazy-paving, 63.8% consolidations, 57.5% stripes and 76.6% air bronchograms. Two cases presented pulmonary nodules. No cavities, pleural effusions nor enlarged mediastinal lymphadenopathies were detected. Bilateral pulmonary involvement took place in 78.7% of cases and concerned mainly the lower lobes (left lower lobe 85.1%, right lower lobe 72.3%). Peripheral subpleural distribution was described in 93.6% of patients; among them 25.5% displayed associated peribronchovascular repartition; 4.3% manifested a prevailing peribronchovascular localization and one severe case manifested diffuse spread [26].

In a single-center retrospective study including 99 real-time RT-PCR confirmed cases of 2019-nCoV in Wuhan Jinyintan Hospital, Chen et al. investigated radiological aspects. Bilateral pneumonia was reported in 74 cases (75%) and pneumothorax occurred in one case (1%) [27].

Gao et al. retrospectively examined high-resolution chest CTs of 6 patients diagnosed with Covid-19. The observed radiological characteristics aligned with those previously reported except one patient who exhibited tree-in-bud sign; an exceptional finding in viral infections that can be viewed in cases of immune disorders [28,29].

Yuan et al. Long et al. and Chung et al. retrospectively studied 27, 36 and 21 chest CTs of patients with confirmed Covid-19 pneumonia, respectively [6,30,31]. Consistently with the aforementioned novel coronavirus (2019-nCoV) infected pneumonia CT features, their findings aligned and included: multiple preponderant ground glass opacities combined with consolidations, predominantly peripheral or in a mixed central and peripheral distribution, bilateral, mainly involving lower lung zones; the right lower lobe being the most frequently concerned [31]; a location possibly favored owing to the right bronchus straight and short anatomical structure. Rarely encountered signs comprised: pure consolidation, sole central distribution, tree-in-bud, cavitation,

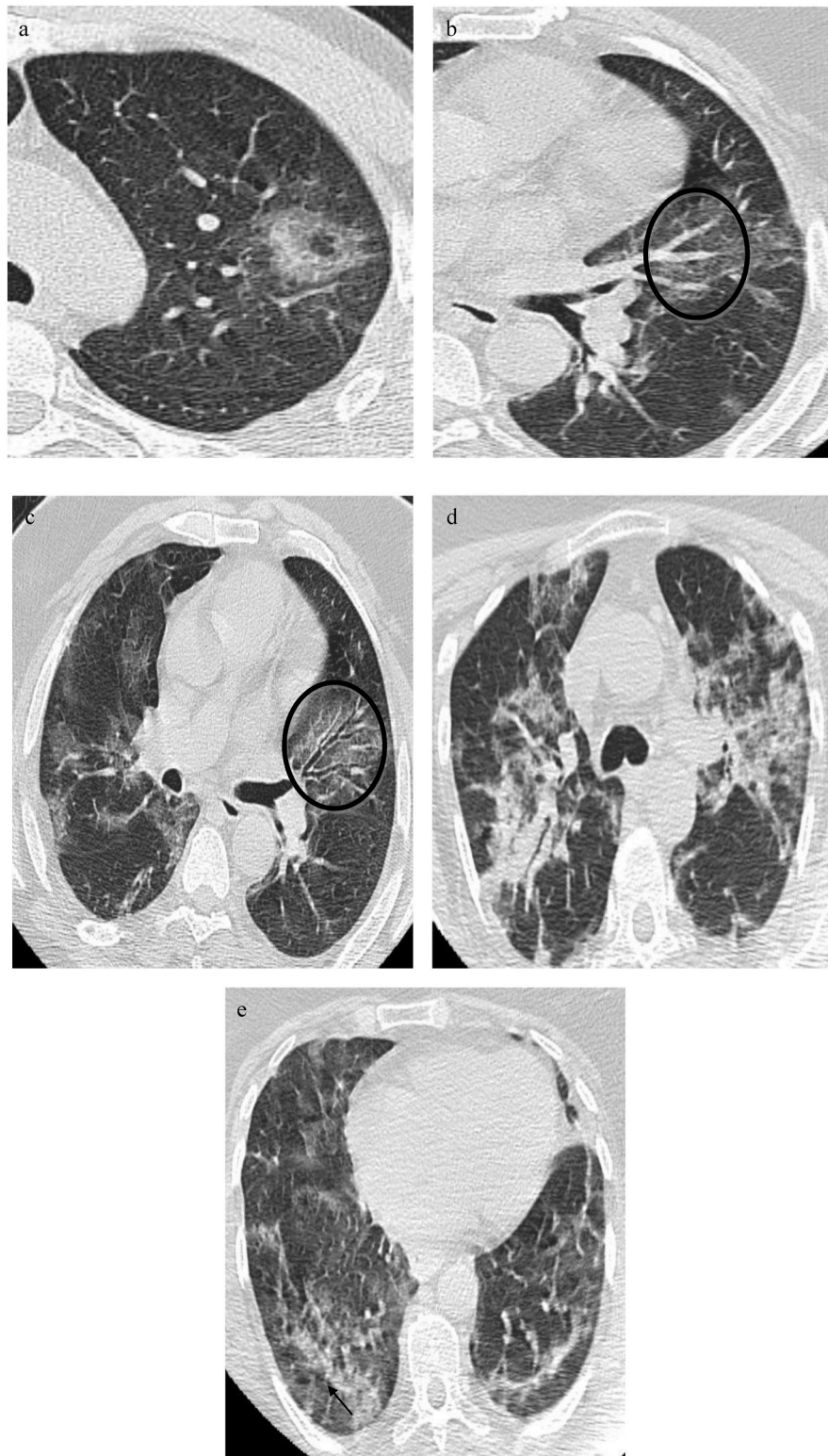


Fig. 1. Covid-19 imaging features in patients with a positive RT-PCR at different disease stages. Unenhanced axial CT images of the lung show.

- (a) A left upper lobe unifocal rounded ground glass opacity;*
- (b) Patchy peripheral ground glass opacity with vascular dilatation (Black circle);*
- (c) Multifocal, bilateral subpleural ground glass opacities with traction bronchiectasis (Black circle);*
- (d) Extensive bilateral ground glass opacities associated with thickened interlobular and intralobular septa (Crazy paving) alongside with peripheral consolidations;*
- (e) Subpleural band in advanced-phase disease (Black arrow).*

mediastinal lymphadenopathy and pleural effusion [6,30,31].

3.2.2. Evolution patterns

Based on the disease phase when scanning is performed, Covid-19

pneumonia's imaging features differ (Fig. 1).

Jin et al. characterized CT findings of five Covid-19 temporal stages. The ultra-early stage; in which asymptomatic patients mainly present sole or several focal ground glass opacities, patchy consolidations,

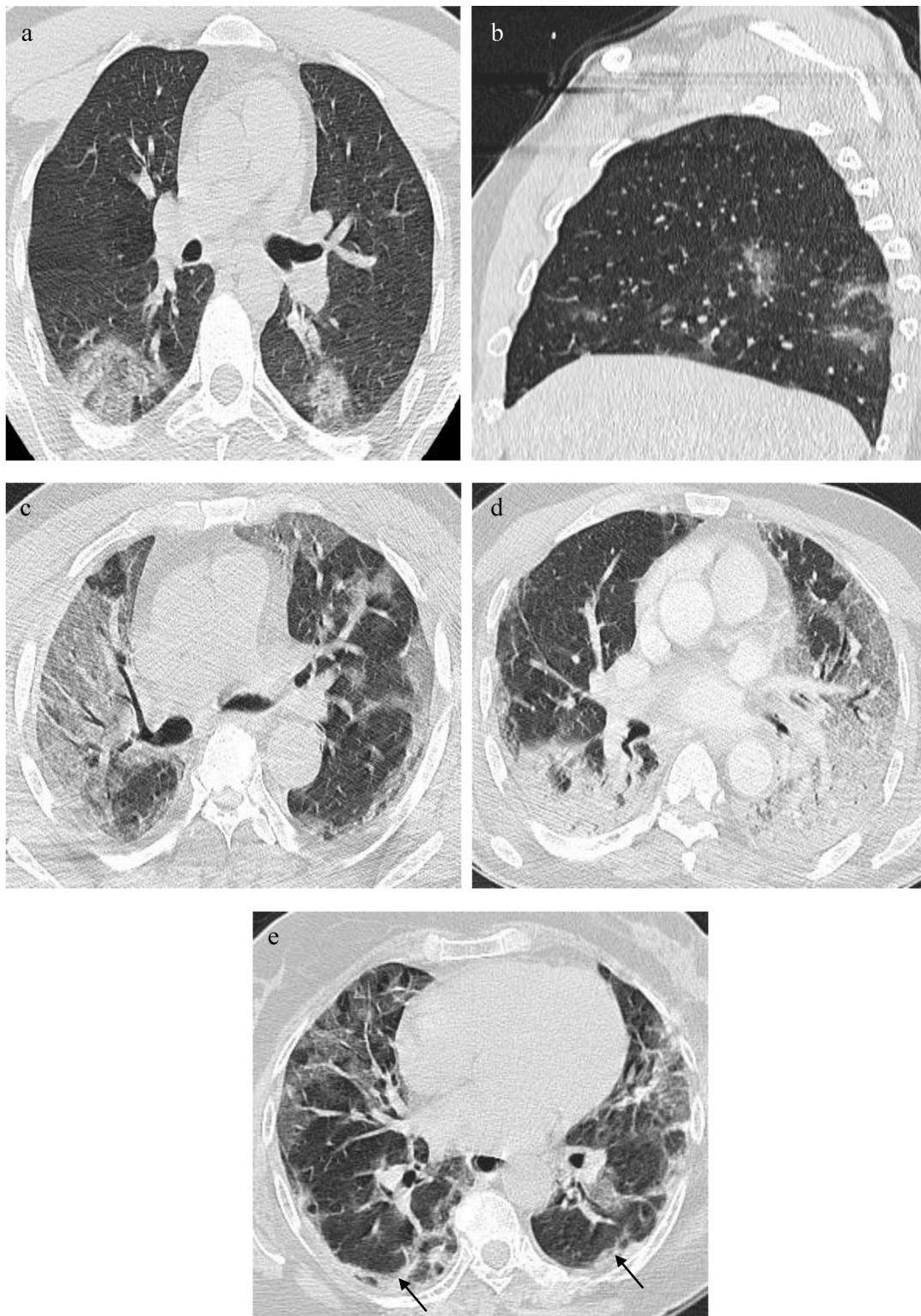


Fig. 2. Covid-19 pneumonia's chest CT imaging features' changes over time.

- (a,b) Early stage: Ground glass opacities involving the lower lobes with partial crazy paving;
- (c) Progressive stage: Ground glass opacities extension and increased crazy paving;
- (d,e) Peak stage: Consolidative opacities, sub-pleural lines (Black arrow) and bronchiectasis.

nodules surrounded by ground glass attenuations and air bronchograms. The early stage (1–3 days after clinical manifestations) where CT exhibits one or numerous ground glass opacities associated with thickened interlobular septa. The rapid progression stage CTs (3–7 days following clinical symptoms) demonstrate sizeable pulmonary consolidative opacities with air bronchograms. The consolidation stage CTs (7–14 days beyond clinical symptoms onset) may show consolidations' extent and density lessening. The dissipation stage (2–3 weeks following onset) is marked by the presence of fewer spotted consolidative opacities, band-like opacities as well as thickened bronchial walls and interlobular septa [32].

In a study including 63 confirmed Covid-19 patients, Pan et al. examined follow-up chest CTs performed 3–14 days after initial examinations. Identified disease progression imaging features included ground glass opacities and consolidations' increase in extent, nodules increase in number, enlargement, confluence and for some, density reduction. Fibrous stripes appearance was associated with recovery whilst a “white lungs” appearance indicated worsening [33].

Pan et al. assessed covid-19's imaging features temporal course in a study including 21 confirmed patients. 4 stages were determined from clinical manifestations onset. In early stage (0–4 days), 4 patients had normal CTs and developed anomalies in the subsequent studies. Uni or bilateral, lower lobes, subpleural ground glass opacities were the major finding. Progressive stage (5–8 days) features consisted of two-sided, multilobar, extensive ground glass attenuations, consolidative opacities and crazy-paving. In peak stage (9–13 days), lesions' extent increased to a peak and dense consolidations prevailed. In absorption stage (14 days), as consolidative opacities and crazy-paving resolved; diffuse ground glass attenuations appeared [34].

Shi et al. grouped 81 Covid-19 patients based on the span separating clinical manifestations onset and the first chest CT. Group 1 (subclinical patients) presented prevailing one-sided multifocal ground glass attenuations. Group 2 (≤ 1 week following symptoms) showed two-sided extensive abnormalities transitioning from ground glass to consolidative and mixed opacities. Mediastinal lymph nodes enlargement and pleural effusion were noted. Group 3 (> 1 week– ≤ 2 weeks) exhibited consolidative opacities alongside with interstitial alterations (bronchiectasis and thickened interlobular septa) suggestive of fibrosis. Group 4 (> 2 weeks to 3 weeks) findings consisted of predominant consolidative and mixed opacities, pleural thickening/effusion and bronchiolectasis.

Serial CTs demonstrate lung lesions' worsening or amelioration; which helps predict outcome.

The commonest evolution pattern across consecutive CT scans was involvement to a peak point succeeded by radiographic amelioration [35].

A prospective study analyzing 41 Covid-19 patients data reported a median time from symptoms onset to both intensive care unit admission and assisted artificial ventilation of 10.5 days (IQR 8.0–17.0) and 10.5 days (IQR 7.0–14.0), respectively [36] (Fig. 2).

3.2.3. Correlation with histopathological anomalies

The small sized virions deposit on the peripheral lung lobules leading to alveolar epithelium sloughing and alveolar wall break-down thus substituting the alveoli by exsudates, hyaline membrane, epithelium and cell debris. Interstitium hyperplasia, bronchioles edema, vascular congestion and microthrombi occur as well; all impacting several adjoining lobules [37–41].

In SARS' acute phase (< 11 days), disseminated alveolar damage is noted. In the delayed phase, disseminated alveolar damage, fibrous and organized pneumonia might be seen [42].

On the grounds of pathological alterations of SARS-Cov pulmonary infection; ground glass opacities may be the result of fractional airspaces filling. Consolidation may be consequent to disseminated alveolar damage, whilst bands spring from interstitial thickening or fibrosis [42].

3.2.4. Severity

Critically ill patients' chest CTs demonstrate two-sided subsegmental and multi-lobar consolidations [4]. Over the course of a few days, rapid progression is noted and scans may exhibit ‘white lungs’ appearance [1].

Yuan et al. investigated radiologic features association with mortality in a retrospective study including 27 patients with confirmed novel coronavirus 2019 infected pneumonia. In the mortality group; extensive and rapidly progressive multilobar consolidative opacities were present; indicating grave clinical evolution [30]. Pathologically, they correspond to diffuse alveolar injury, a recognized poor prognosis marker in H1N1, H5N1, H7N9 and SARS pneumonias [30,43,44] (Fig. 3).

3.2.5. Complications

Supplemental oxygen requirements raise suspicion of complications and indicate repeat CTs. CT identifies signs of Covid-19 myocardial injury induced pulmonary edema, superinfection, pulmonary thromboembolism when contrast-enhanced, progression towards acute respiratory distress syndrome and pneumothorax under mechanical ventilation ... [45] (Fig. 4).

3.2.6. Systematic reviews and meta-analysis reporting COVID-19 pneumonia's imaging features

Covid-19 pneumonia's imaging features have been extensively investigated. Among 72 systematic reviews and meta-analyses retrieved from pubmed, 20 were summarized in Table 1, based on the following criteria: recent articles published in english, and including patients with confirmed Covid-19 infection, large sample size, sufficient imaging data, and rigorous study design. High statistical heterogeneity was noted, due probably to differences in patient populations and study settings.

In a study involving 919 patients, Salehi et al. report the following initial characteristic CT aspects: multilobar, bilateral, principally in the lower lobes, peripherally distributed ground glass opacification. Later, in the intermediate course of the disease, ground glass opacities increase in size and number gradually turning into multifocal consolidations. Septal thickening and crazy-paving develop [4]. Mixed ground glass opacities and consolidations are frequently found. Septal thickening, bronchiectasis and pleural thickening are less common. Pleural effusion, pericardial effusion, mediastinal lymphadenopathy, cavities, halo sign and pneumothorax are rare however possible; detected with disease progression. In certain studies; Covid-19 CT features differed in relation to age with older patients presenting more atypical findings and consolidative opacities than younger ones in which ground glass attenuations prevailed [4,62,63].

In a systematic review and meta-analysis including 46 959 patients, Cao et al. reported the following two main chest CT aspects: bilateral lung involvement (75.7%, 0.639–0.871) and ground glass opacities (69.9%, 0.602–0.796), followed by halo sign (54.4%, 0.255–0.833), air bronchograms (51.3%, 0.326–0.701), thickening of bronchovascular bundles (39.5%, 0.082–0.708), grid-like shadows (24.4%, 0.116–0.371) and hydrothorax (18.5%, 0.001–0.370). Nodules, stripes, vascular enhancement sign, bronchial wall thickening, anti-halo and mosaic signs ... were also described [1].

In a scoping review and meta-analysis of 59 254 patients imaging data, Borges do Nascimento et al. stated that the most frequently encountered abnormalities amongst patients who undertook chest radiography were bilateral opacities, multifocal ground glass shadows, infiltrations and consolidations. 6 patients presented normal chest films.

Concerning computed tomography: 8 patients had normal CTs. Predominantly bilateral, peripheral, patchy ground glass opacities prevailed (associated or not with thickened septa), succeeded by consolidations. Ground glass nodules' size increase and progression to alveolar consolidations were of note [2].

Rodriguez-Morales et al. reported Covid-19 pneumonia main chest x-rays features in a systematic review and meta-analysis comprising 2874 patients. Their findings consisted of bilateral pneumonia and ground

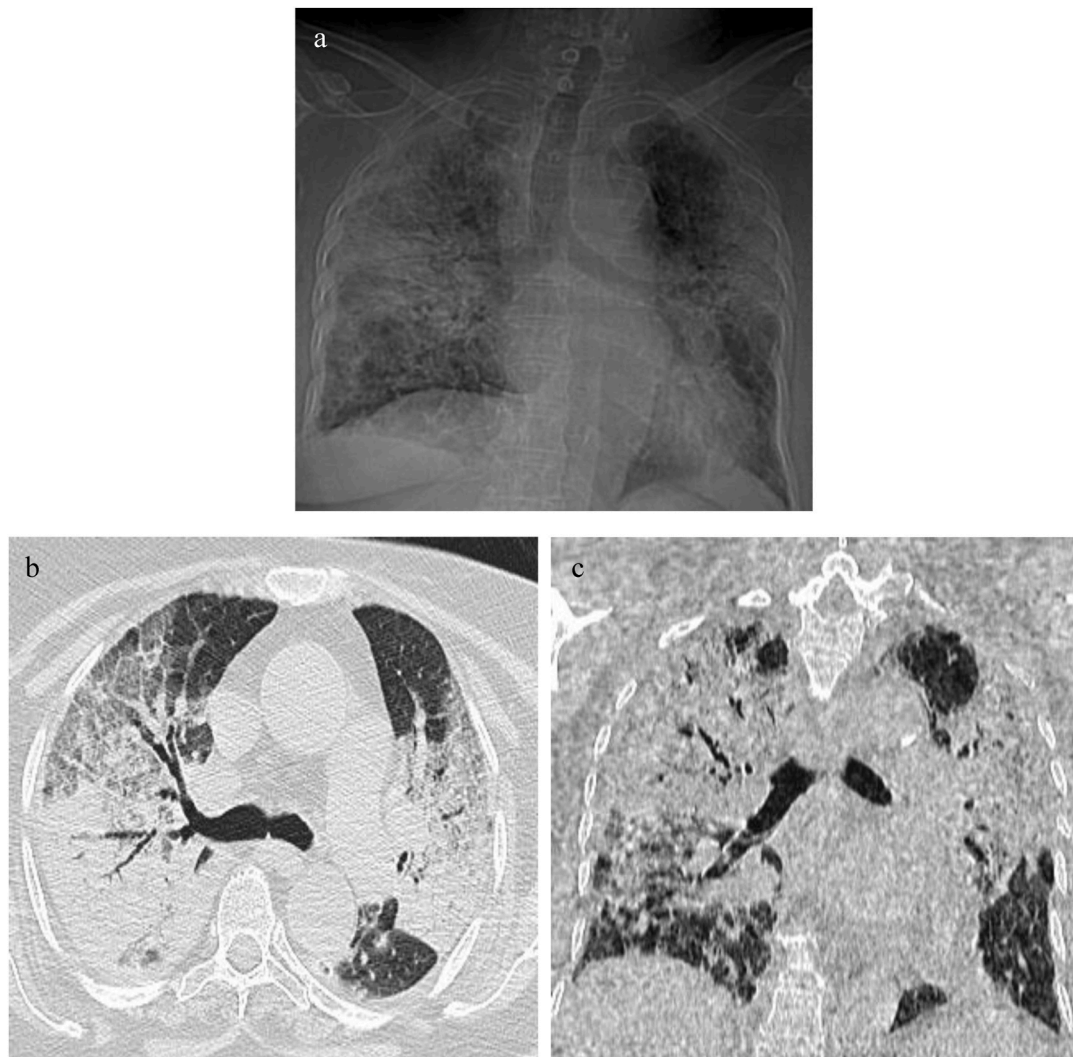


Fig. 3. A 40 year-old-patient with a history of ten days of fever and coughing presented to the emergency department with an 86% O₂ saturation and a 32/min respiratory rate. Frontal chest radiography (a) revealed extensive multilobar consolidations. Chest CT axial (b) and coronal (c) images showed typical severe peak-stage Covid-19 pneumonia imaging features with extensive ground glass opacities, crazy paving pattern, multilobar consolidations and bronchiectasis.



Fig. 4. Axial chest CT image in a patient with severe advanced stage Covid-19 pneumonia complicated by right pneumothorax, pneumomediastinum and subcutaneous emphysema under mechanical ventilation.

glass opacities [3].

3.3. Diagnostic difficulties and differentials

In the presence of immune disorders or underlying pulmonary diseases (emphysema, fibrosis ...), atypical Covid-19 imaging patterns can be observed and diminish diagnostic confidence [64]. Covid-19 temporal progression is another noteworthy element to take into account. Early (first two days after symptoms onset) negative CTs should not be relied on to exclude the presence of SARS-CoV 2 infection [33,65].

Although highly sensitive in diagnosing Covid-19 pneumonia, chest CT features in a screening population are non-specific [14]. Infectious (viral and bacterial pneumonia ...) as well as non-infectious diseases (vasculitis, organizing pneumonia ...) share Covid-19 imaging features complicating the differential diagnosis [66]. Viral pneumonia (Influenza A virus, Influenza B virus, SARS-CoV, MERS coronavirus cytomegalovirus, adenovirus, respiratory syncytial virus ...) primarily exhibits interlobular septa, peri-bronchial and peri-vascular interstitial inflammation. On CT, numerous hilar and subpleural high attenuation reticulations are noted [67,68]. Bronchial wall inflammation clogs the bronchioles in part or in total and appears as focal edema or atelectasis on CT.

Covid-19 imaging features resemble those of SARS and MERS [69,

Table 1
Summary of systematic reviews and meta-analysis key findings.

| Author/Year/Journal | Article type | Imaging modality | Key findings | Number of studies | Number of patients | Age (y-Old) | Effect estimate [95% CI] | P value | Heterogeneity (I ²)% | P value | P value of publication bias tests | |
|--|-------------------------------------|--------------------|--|--------------------|---------------------------------------|---------------------|--------------------------|---------|----------------------------------|---------|-----------------------------------|--|
| Zarifian et al [46]. February 2020 Clinical imaging | Systematic review and meta-analysis | Chest CT | <u>Imaging findings</u> | 103 | 9907 | | | | | | | |
| | | | GGO±consolidation | 66 | 6224 | | 0.771(0.722-0.814) | | 89.5 | | 0.001 | |
| | | | Reticulation±GGO | 41 | 2667 | | 0.462(0.385-0.541) | | 90.21 | | 0.652 | |
| | | | Consolidation | 44 | 4397 | | 0.355(0.288-0.429) | | 96.06 | | 0.825 | |
| | | | Organizing pneumonia | 33 | 2557 | | 0.368(0.289-0.455) | | 92.25 | | 0.912 | |
| | | | Pleural effusion | 48 | 3963 | | 0.069(0.050-0.094) | | 78.25 | | 0.001 | |
| | | | Lymphadenopathy | 39 | 3197 | | 0.051(0.035-0.075) | | 88.05 | | 0.001 | |
| | | | <u>Distribution</u> | | | | | | | | | |
| | | | Bilateral distribution | 70 | 5505 | | 0.757(0.707-0.800) | | 89.78 | | 0.602 | |
| | | | Central | 26 | 2160 | | 0.061(0.038-0.094) | | 91.73 | | 0.001 | |
| Diffuse | 28 | 2080 | | 0.351(0.267-0.444) | | 89.54 | | 0.069 | | | | |
| Peripheral | 43 | 3216 | | 0.656(0.582-0.723) | | 94.29 | | 0.002 | | | | |
| Middle lobe | 15 | 1487 | | 0.478(0.354-0.606) | | 94.44 | | 0.004 | | | | |
| Rodriguez-Morales et al [3]. March 2020 Travel Medicine and Infectious Disease | Systematic review and meta-analysis | Chest x-ray | <u>Pneumonia compromise</u> | 19 | 2874 | 51.97 | | | | | Egger's test P=0.801 | |
| -Unilateral pneumonia | | | 7 | 316 | (46.06–57.89) | 0.25(0.052-0.448) | <0.001 | 96.37 | | | | |
| -Bilateral pneumonia | | | 9 | 557 | | 0.729 (0.586-0.871) | <0.001 | 98.28 | | | | |
| | | | <u>Imaging findings</u> | | | | | | | | | |
| | | | -Ground glass opacities | 10 | 584 | | 0.68(0.518-0.852) | <0.001 | 99.09 | | | |
| Borges do Nascimento et al [2]. April 2020 Journal of clinical medicine | Scoping review and meta-analysis | Chest x-ray | Uni or bilateral chest opacities ± pleural effusion | 61 | 59 254 22 | 3 months-99 years | | | | | | |
| | | Chest CT | Multiple GGO Infiltrate Normal findings GGO (± septal thickening) Infiltration abnormalities Parenchymal consolidation Normal CT | | 20 4 6 1204 9 325 8 | | | | | | | |
| Sun et al [47]. May 2020 Quantitative Imaging in Medicine and Surgery | Systematic review and meta-analysis | Chest x-ray and CT | <u>Lesions' distribution</u> | 55 | 6616 | 48 (45.1–50.9) | | | | | | |
| Bilateral involvement | | | | | | 0.780(0.450-1) | | <0.001 | | | | |
| Unilateral involvement | | | | | | 0.203(0.099-0.300) | | <0.001 | | | | |
| Peripheral distribution | | | | | | 0.653(0.259-1) | | <0.001 | | | | |
| Central distribution | | | | | | 0.035(0.009-0.098) | | <0.001 | | | | |
| Peripheral & central distribution | | | | 0.311(0.019-0.740) | | 0.102 | | | | | | |

(continued on next page)

Table 1 (continued)

| Author/Year/Journal | Article type | Imaging modality | Key findings | Number of studies | Number of patients | Age (y-Old) | Effect estimate [95% CI] | P value | Heterogeneity (I ²)% | P value | P value of publication bias tests |
|--|---|------------------|--|-------------------|---|-------------|---|---------|----------------------------------|----------------------|-----------------------------------|
| | | | <u>Imaging findings</u> | | | | | | | | |
| | | | Normal imaging | | | | 0.133(0.007-0.384) | | | <0.001 | |
| | | | GGO | | | | 0.580(0.166-1) | | | <0.001 | |
| | | | Consolidation | | | | 0.441(0.016-0.714) | | | <0.001 | |
| | | | GGO & consolidation | | | | 0.529(0.190-0.767) | | | <0.001 | |
| | | | Interlobular septal thickening | | | | 0.229(0.009-0.804) | | | <0.001 | |
| | | | Crazy-paving pattern | | | | 0.235(0.031-0.916) | | | <0.001 | |
| | | | Pleural effusion | | | | 0.110(0.009-0.804) | | | <0.001 | |
| | | | Air bronchogram | | | | 0.425(0.077-0.803) | | | <0.001 | |
| | | | Lymphadenopathy | | | | 0.048(0.009-0.084) | | | 0.084 | |
| | | | Nodules | | | | 0.116(0.020-0.428) | | | <0.001 | |
| | | | Linear opacity | | | | 0.412(0.074-0.650) | | | <0.001 | |
| Chang et al [48]. May 2020 Journal of the Formosan Medical Association | Systematic review and meta-analysis | Chest CT | Patchy consolidations Ground glass opacities No lesion | 3 | 93 | | 0.31(0.13-0.55) 0.48(0.36-0.64) 0.27(0.18-0.43) | | 51 0 0 | 0.09 0.52 0.64 | |
| Elshafeey et al [49]. July 2020 International journal of gynecology and obstetrics | Systematic scoping review | Chest CT | <u>Lesion's distribution</u> Bilateral pneumonia Unilateral pneumonia | 33 | 385 99/125 (79.2%) 22/125 (17.6%) | 21-42 | | | | | |
| | | | <u>Imaging findings</u> No lesions | | 4/125 (3.2%) | | | | | | |
| | | | GGO | | 102/125 (81.6%) | | | | | | |
| | | | Consolidation | | 22/125 (17.6%) | | | | | | |
| | | | Reticular | | 1/125 (0.8%) | | | | | | |
| | | | Pleural thickening | | 1/125 (0.8%) | | | | | | |
| | | | Pleural effusion | | 9/125 (7.2%) | | | | | | |
| | | | Atelectasis | | 1/125 (0.8%) | | | | | | |
| | | | Crazy-paving | | 1/125 (0.8%) | | | | | | |
| Salehi et al [4]. July 2020 American Journal of Roentgenology | Systematic review | Chest CT | <u>Lesions' distribution</u> Bilateral involvement Peripheral distribution | 30 12 12 | 919 435/497 (87.5%) 92/121 (76%) | | | | | | |

(continued on next page)

Table 1 (continued)

| Author/Year/Journal | Article type | Imaging modality | Key findings | Number of studies | Number of patients | Age (y-Old) | Effect estimate [95% CI] | P value | Heterogeneity (I ²)% | P value | P value of publication bias tests | | | | |
|--|-------------------------------------|-------------------------------------|--|-------------------|--------------------|----------------------------|--------------------------|-----------------|----------------------------------|---------|--|--------|--------|--|--|
| Kumar et al [50]. July 2020 Journal of tropical pediatrics | Systematic review and meta-analysis | Chest CT Chest x-ray Chest US | Posterior involvement | 1 | 41/51 (80.4%) | | | | | | Considered high (all the included studies were either case series or case reports) | | | | |
| | | | Multilobar involvement | 5 | 108/137 (78.8%) | | | | | | | | | | |
| | | | <u>Imaging findings</u> | | | | | | | | | | | | |
| | | | GGO | 22 | 346/393 (88%) | | | | | | | | | | |
| | | | Consolidation | 10 | 65/204 (31.8%) | | | | | | | | | | |
| | | | GGO | 32 | 706 | | | | 0.39(0.31-0.48) | | | 82 | 0.00 | | |
| | | | Consolidation | 12 | 192 | | | | 0.23(0.12-0.34) | | | 82 | 0.00 | | |
| | | | Halo sign | 6 | 78 | | | | 0.26(0.11-0.41) | | | 51 | 0.09 | | |
| | | | Patchy shadow | 13 | 246 | | | | 0.44(0.32-0.55) | | | 62 | 0.00 | | |
| | | | Prominent bronchovascular markings | 5 | 97 | | | | 0.17(0.09-0.24) | | | 0.0 | 0.83 | | |
| | | | Bronchial wall thickening | 4 | 36 | | | | 0.11(0.01-0.21) | | | 0.0 | 1.00 | | |
| | | | Pleural effusion | 5 | 187 | | | | 0.02(0.001-0.04) | | | 0.0 | 0.60 | | |
| | | | Interstitial pattern | 4 | 187 | | | | 0.12(0.01-0.23) | | | 82 | 0.00 | | |
| | | | Nodules | 5 | 63 | | | | 0.25(0.09-0.41) | | | 62 | 0.03 | | |
| Cao et al [1]. September 2020 Journal of medical virology | Systematic review and meta-analysis | Chest CT | <u>Pneumonia compromise</u> | 31 | 46 95 | 46.62 (31.71-61.53) | 0.201(0.106-0.302) | <0.001 | 97.605 | <0.001 | Egger's test P =0.091 | | | | |
| | | | Unilateral pneumonia | | 522 | | 0.755(0.639-0.871) | <0.001 | 98.736 | <0.001 | | | | | |
| | | | Bilateral pneumonia | | 1196 | | | | | | | | | | |
| | | | <u>Imaging findings</u> | | | | | | | | | | | | |
| | | | Lung consolidation | | 122 | | | | 0.369(0.215-0.523) | <0.001 | | 91.717 | <0.001 | | |
| | | | Ground-glass | | 1413 | | | | 0.699(0.602-0.796) | <0.001 | | 98.651 | <0.001 | | |
| | | | Air bronchogram | | 119 | | | | 0.513(0.326-0.701) | <0.001 | | 89.834 | <0.001 | | |
| | | | Grid-form shadow | | 64 | | | | 0.244(0.116-0.371) | <0.001 | | 87.365 | <0.001 | | |
| | | | Bronchovascular bundles thickening | | 41 | | | | 0.395(0.082-0.708) | 0.013 | | 95.592 | <0.001 | | |
| | | | Hydrothorax | | 23 | | | | 0.185(0.001-0.370) | 0.049 | | 97.871 | <0.001 | | |
| | | | Irregular or halo sign | | 107 | | | | 0.544(0.255-0.833) | <0.001 | | 96.217 | <0.001 | | |
| | | | Cui et al [51]. September 2020 Journal of medical virology | Review | Chest CT | <u>Imaging findings</u> | 24 | 2597 | < 1 year: 446 (17.9%) | | | | | | |
| | | | | | | Normal imaging | | 178/409 (43.5%) | 1 -5 years: 593 (23.8%) | | | | | | |
| | | | | | | Ground-glass opacity | | 87/294 (29.6%) | 6 - 10 years: 626 (25.1%) | | | | | | |
| Local patchy shadowing | | 60/294 (20.4%) | | | | 11 - 15 years: 492 (19.7%) | | | | | | | | | |
| Bilateral patchy shadowing | | 43/294 (14.6%) | | | | >15 years: 335 (13.4%) | | | | | | | | | |
| White lung change | | 2/409 (0.5%) | | | | | | | | | | | | | |
| Pleural effusion | | 3/409 (0.7%) | | | | | | | | | | | | | |

(continued on next page)

Table 1 (continued)

| Author/Year/Journal | Article type | Imaging modality | Key findings | Number of studies | Number of patients | Age (y-Old) | Effect estimate [95% CI] | P value | Heterogeneity (I ²)% | P value | P value of publication bias tests |
|---|-------------------------------------|------------------|--------------------------------|-------------------|--------------------|-------------|--------------------------|---------|----------------------------------|---------|-----------------------------------|
| Wan et al [52]. July 2020 Academic radiology | Systematic review and meta-analysis | Chest CT | <u>Imaging findings</u> | 14 | 1115 | 48.02 | | | | | |
| | | | GGO | 13 | 1073 | | 0.690(0.580-0.800) | | 96.7 | | |
| | | | Consolidation | 14 | 1115 | | 0.470(0.350-0.600) | | 95.6 | | |
| | | | Air bronchogram | 8 | 565 | | 0.460(0.250-0.660) | | 97.6 | | |
| | | | Crazy-paving | 7 | 695 | | 0.150(0.080-0.220) | | 89.1 | | |
| | | | <u>Extent</u> | | | | | | | | |
| | | | RLL | 8 | 547 | | 0.700(0.460-0.950) | | 98.6 | | |
| | | | ≥3 lobes | 7 | 438 | | 0.650(0.580-0.730) | | 63 | | |
| | | | All 5 lobes involved | 8 | 489 | | 0.420(0.320-0.530) | | 84.4 | | |
| | | | <u>Distribution</u> | | | | | | | | |
| Awulachew et al [53]. July 2020 Radiology Research and Practice | Systematic review and meta-analysis | Chest CT | <u>Imaging finding</u> | 60 | 5041 | 49±11.6 | | | | | 0.1947 |
| | | | GGO with consolidation | | 768 (18%) | | | | | | |
| | | | GGO | | 2482 (65%) | | | | | | |
| | | | Consolidation | | 1259 (22%) | | | | | | |
| | | | Crazy-paving | | 575(12%) | | | | | | |
| | | | Reversed halo sign | | 146(1%) | | | | | | |
| | | | Interlobular septal thickening | | 691(27%) | | | | | | |
| | | | Air bronchogram sign | | 531(18%) | | | | | | |
| | | | <u>Distribution</u> | | | | | | | | |
| | | | Bilateral | | 3952 (80%) | | | | | | |
| | | | Unilateral | | 641(20%) | | | | | | |
| | | | Right lung | | 48(62%) | | | | | | |
| | | | Left lung | | 29(38%) | | | | | | |
| | | | LUL | | 731(74%) | | | | | | |
| | | | LLL | | 504(46%) | | | | | | |
| | | | RUL | | 455(40%) | | | | | | |
| | | | RML | | 326(38%) | | | | | | |
| | | | RLL | | 784(74%) | | | | | | |
| | | | <u>Extent</u> | | | | | | | | |
| | | | One lobe | | 278(14%) | | | | | | |
| Two lobes | | 299(11%) | | | | | | | | | |
| Three lobes | | 250(13%) | | | | | | | | | |
| 4 lobes | | 212(15%) | | | | | | | | | |
| 5 lobes | | 384(34%) | | | | | | | | | |
| >one lobe | | 1145 (76%) | | | | | | | | | |
| <u>Other findings</u> | | | | | | | | | | | |
| Pleural effusion | | | 94(1.6%) | | | | | | | | |
| Lymphadenopathy | | | 21(0.7%) | | | | | | | | |
| Pulmonary nodules | | | 262(9%) | | | | | | | | |
| <u>Follow-up findings</u> | | | | | | | | | | | |

(continued on next page)

Table 1 (continued)

| Author/Year/Journal | Article type | Imaging modality | Key findings | Number of studies | Number of patients | Age (y-Old) | Effect estimate [95% CI] | P value | Heterogeneity (I ²)% | P value | P value of publication bias tests | | |
|--|-------------------------------------|------------------|---|-------------------|--------------------|-------------|--------------------------|---------|----------------------------------|---------|-----------------------------------|--------------------|------|
| Jutzeler et al [54]. August 2020 Travel Medicine and Infectious Disease | Systematic review and meta-analysis | Chest CT | Early disease : Pure GGO followed by Crazy-paving Later disease course : Consolidation, prominent bilateral involvements | 148 | 12'149 | 47(35-64.4) | 0.691(0.568-0.792) | | 97.9 | | Egger's test: p < 0.05 | | |
| | | | <u>Imaging findings</u> GGO | 62 | 2446/5591 | | | | | | | | |
| | | | Consolidation | 30 | 771/2022 | | | | | | | 0.383(0.269-0.511) | 92.1 |
| | | | GGO with consolidation | 15 | 153/323 | | | | | | | 0.495(0.405-0.587) | 43.1 |
| | | | Nodular lesions | 13 | 70/1345 | | | | | | | 0.153(0.073-0.295) | 83.3 |
| | | | Reticulation/interlobular septal thickening | 7 | 81/1244 | | | | | | | 0.218(0.051-0.593) | 95.8 |
| | | | Crazy-paving pattern | 5 | 59/210 | | | | | | | 0.307(0.138-0.550) | 75.2 |
| | | | Pleural effusion | 10 | 2745/4247 | | | | | | | 0.078(0.050-0.121) | 94.6 |
| | | | <u>Lesions' distribution</u> Bilateral pneumonia | 48 | 52/666 | | | | | | | 0.772(0.708-0.831) | 55.6 |
| | | | Unilateral pneumonia | 32 | 799/3745 | | | | | | | 0.192(0.164-0.224) | 73 |
| Mouhand F. et al [55]. August 2020 The American journal of tropical medicine and hygiene | Systematic review and meta-analysis | Lung US | <u>Imaging findings</u> B-pattern | 7 | 122 | >18years | 0.97 | | 0 | | | | |
| | | | Pleural line abnormalities | 7 | | | (0.94–1.00) | | | | | | |
| | | | Pleural thickening | 5 | | | 0.70 | | | | | 96 | |
| | | | | 5 | | | (0.13–1.00) | | | | | 0.54 | 93 |
| | | | Subpleural or pulmonary consolidation | 6 | | | 0.39 | | | | | 72 | |
| | | | Pleural effusion | 5 | | | (0.21–0.58) | | | | | 0.14 | 93 |
| | | | (0.00–0.37) | | | | | | | | | | |
| Syed Zaki et al [56]. September 2020 Le Infezioni in Medicina | Systematic review and meta-analysis | Chest CT | <u>Distribution of lesion</u> -Bilateral | 54 | 2693 | | 0.741(0.684-0.795) | | 85.76 | | | | |
| | | | -Subpleural | | 299/509 | | 0.572(0.390-0.743) | | | | | 93.08 | |
| | | | -Peripheral | | 770/1287 | | 0.571(0.467-0.671) | | | | | 92.42 | |
| | | | -Posterior | | 44/69 | | 0.379(0.015-0.872) | | | | | 92.38 | |
| | | | -Unilateral | | 216/1048 | | 0.205(0.150-0.266) | | | | | 77.48 | |
| | | | -Central | | 47/551 | | 0.089(0.031-0.172) | | | | | 87.84 | |
| | | | <u>Lobe involvement</u> -LLL | | 500/696 | | 0.715(0.589-0.821) | | | | | 90.91 | |
| | | | -RLL | | 504/710 | | 0.665(0.534-0.785) | | | | | 91.45 | |
| | | | | | | | | | | | | | |
| | | | | | | | | | | | | | |

(continued on next page)

Table 1 (continued)

| Author/Year/Journal | Article type | Imaging modality | Key findings | Number of studies | Number of patients | Age (y-Old) | Effect estimate [95% CI] | P value | Heterogeneity (I ²)% | P value | P value of publication bias tests |
|--|-------------------------------------|------------------|------------------------------|-------------------|--------------------|-------------|--------------------------|---------|----------------------------------|---------|---|
| | | | -LUL | | 403/681 | | 0.572(0.444-0.694) | | 90.39 | | |
| | | | -RUL | | 385/690 | | 0.531(0.418-0.642) | | 87.66 | | |
| | | | -RML | | 345/736 | | 0.428(0.291-0.571) | | 93.24 | | |
| | | | <u>Imaging findings</u> | | | | | | | | |
| | | | GGO | | 1541/2416 | | 0.646(0.576-0.714) | | 91.52 | | |
| | | | Mixed | | 524/1176 | | 0.430(0.368-0.493) | | 72.56 | | |
| | | | Consolidation | | 615/2037 | | 0.277(0.191-0.371) | | 95.19 | | |
| | | | Septal thickening | | 399/846 | | 0.406(0.282-0.537) | | 92.74 | | |
| | | | Air bronchogram | | 491/1199 | | 0.397(0.291-0.509) | | 93.26 | | |
| | | | Fibrosis/stripes | | 200/562 | | 0.372(0.217-0.541) | | 93.98 | | |
| | | | Crazy-paving | | 350/1181 | | 0.290(0.190-0.401) | | 93.68 | | |
| | | | Subpleural lines | | 117/698 | | 0.150(0.072-0.251) | | 90.81 | | |
| | | | Nodules | | 95/918 | | 0.112(0.065-0.170) | | 83.28 | | |
| | | | Pleural effusion | | 108/1784 | | 0.058(0.041-0.077) | | 62.31 | | |
| | | | Lymphadenopathy | | 65/1193 | | 0.053(0.029-0.084) | | 72.11 | | |
| | | | Pericardial effusion | | 13/394 | | 0.030(0.013-0.054) | | 33.16 | | |
| Xu et al [57]. October 2020 European radiology | Systematic review and meta-analysis | Chest CT | Sensitivity | 16 | 3186 | 37-62 | 0.92(0.86-0.96) | | 96.4 | | The risks of bias in all studies were moderate. |
| | | | Specificity | 14 | 2689 | | 0.25(0.22-0.3) | | | | |
| Choi et al [58]. November 2020 European journal of radiology | Systematic review and meta-analysis | Brain CT and MRI | Cerebral microhemorrhages | 21 | 2125 | >58 years | 0.33(0.23-.44) | <0.001 | 94 | | <0.001 |
| | | | Spontaneous acute ICH | | | | 0.054(0.031-0.076) | <0.001 | 87 | | <0.001 |
| | | | Acute/subacute infarct | | | | 0.240(0.160-0.318) | <0.001 | 97 | | 0.014 |
| | | | Encephalitis/encephalo-pathy | | | | 0.330(0.019-0.047) | <0.001 | 92 | | <0.001 |
| Garg et al [59]. November 2020 Clinical Imaging | Systematic review and meta-analysis | Chest x-ray | <u>Imaging findings</u> | 56 | 6007 | 2.1-70 | | | | | |
| | | Chest CT | GGO | 5 | 396 | | 0.387(0.222-0.583) | | 83 | | |
| | | | Consolidation | | 5762 | | 0.469-0.297-0.649) | | 84 | | |
| | | | <u>Imaging findings</u> | | | | | | | | |
| | | | GGO | | | | 0.669(0.608-0.724) | | 92 | | |
| | | | GGO+Consolidations | | | | 0.449(0.387-0.513) | | 83 | | |
| | | | Consolidation | | | | | | 96 | | |

(continued on next page)

Table 1 (continued)

| Author/Year/Journal | Article type | Imaging modality | Key findings | Number of studies | Number of patients | Age (y-Old) | Effect estimate [95% CI] | P value | Heterogeneity (I ²)% | P value | P value of publication bias tests |
|--|-------------------------------------|------------------|---|-------------------|--------------------|-----------------|---------------------------------|---------|----------------------------------|---------|-----------------------------------|
| | | | | | | | 0.321(0.236-0.419) | | | | |
| | | | Crazy-paving | | | | 0.291(0.196-0.408) | | 93 | | |
| | | | Halo sign | | | | 0.236(0.117-0.418) | | 94 | | |
| | | | Nodule | | | | 0.089(0.057-0.138) | | 65 | | |
| | | | Pleural effusion | | | | 0.056(0.042-0.074) | | 51 | | |
| | | | Lymphadenopathy | | | | 0.027(0.013-0.055) | | 84 | | |
| | | | <u>Diagnostic accuracy estimates</u> | | | | | | | | |
| | | | GGO sensitivity/specificity | | | | 0.73(0.71-0.80)/0.61(0.41-0.78) | | 96/94 | | |
| | | | GGO+Consolidation sensitivity/specificity | | | | 0.58(0.48-0.68)/0.58(0.41-0.73) | | 31/77 | | |
| | | | Consolidation only sensitivity/specificity | | | | 0.49(0.20-0.78)/0.56(0.30-0.78) | | 96/91 | | |
| Islam et al [60]. December 2020 Frontiers in medicine. | Review | Chest CT | Early identification Reduces transmission especially in asymptomatic patients <u>Imaging findings</u> GGO Patch-like shadows Fiber shadows Pleural effusion Pleural thickening <u>Distribution</u> Bilateral, multi-lobe distribution Peripheral, random, and diffuse involvement | 13 | 235 | 25-40 | | | | | |
| Nino et al [61]. January 2021 Pediatric Pulmonology | Systematic review and meta-analysis | Chest CT | <u>Imaging findings</u> Normal imaging GGO Consolidations/pneumonic infiltrates <u>Distribution</u> Bilateral compromise | 29 | 1026 | 6.57 (1.5–14.5) | 0.375(0.275-0.440) | <0.001 | 86.31 | | |
| | | | | | | | 0.372(0.293-0.450) | <0.001 | 85.76 | | |
| | | | | | | | 0.223(0.178-0.269) | <0.001 | 94.54 | | |
| | | | | | | | 0.277(0.199-0.356) | <0.001 | 87.59 | | |

70]. One could theorize that the SARS-CoV2 infected pulmonary parenchyma might react in a way comparable to the SARS and MERS lung recovery patterns [71]. Shared features are peripheral ground glass and consolidative opacities combined with crazy-paving. SARS usually presents as a unifocal one-sided lung opacity initially [72]. Progression is rapid. Consolidations affect multiple segments and lobes resulting possibly in ‘white lungs’ appearance [73]. Cavities and spontaneous pneumomediastinum are reported [74]. MERS primarily appears as extensive basilar and subpleural ground glass opacities with a scope greater than that of consolidations [75]. Pneumothorax and pleural effusion are common signs and indicate poor prognosis [76].

Bronchial and lobar pneumonia are bacterial pneumonias major manifestations. Their CT features comprise extensive irregular consolidations, mucoid impactions, bronchial walls thickening and centrilobular nodules. Pleural effusion and mediastinal lymphadenopathy are common [19].

Cryptococcus infections manifest as uni or multifocal subpleural nodules and consolidations [77].

Heart failure causes pulmonary alveolar and interstitial edema. Alveolar edema major CT findings are ground glass opacities and high-attenuations typically displaying the butterfly sign. Interstitial edema appears as bilateral interlobular septal thickening, peribronchial

infiltration and blood-flow redistribution [78].

Studies assessing radiologists’ performance in accurately differentiating Covid-19 over other pneumonia on chest-CT are limited. In one investigation, Bai et al. evaluated radiologists accuracy in distinguishing Covid-19 from viral pneumonia; 424 abnormal chest computerized tomographies-among which 219 belonged to patients with RT-PCR confirmed SARS-Cov2 infection and 205 to patients with positive respiratory viral pneumonia-were selected and blindly examined by three chinese radiologists [66]. Their accuracies to differentiate Covid-19 from viral pneumonia were 83% (95 CI: 79–86%), 80% (95% CI: 76–83%), and 60% (95% CI: 55–65%), respectively [48]. In a comparable manner, accuracies of 4 U S radiologists in differentiating covid-19 from non covid-19 pneumonia in 58 age-matched scans chosen at random were 97% (95% CI: 88–100%), 88% (95 CI: 77–95%), 83% (95% CI: 71–91%), and 84% (95% CI: 73–93%), respectively. Specificity fluctuated from 93 to 100% and sensitivity from 70 to 93%. Authors concluded that chinese and U.S radiologists sensitivity to discriminate Covid-19 pneumonia from viral pneumonia on chest CT was moderate whilst specificity was high. Of note, the cohort size was small and non-infectious diseases with Covid-19 comparable features were not integrated [66].

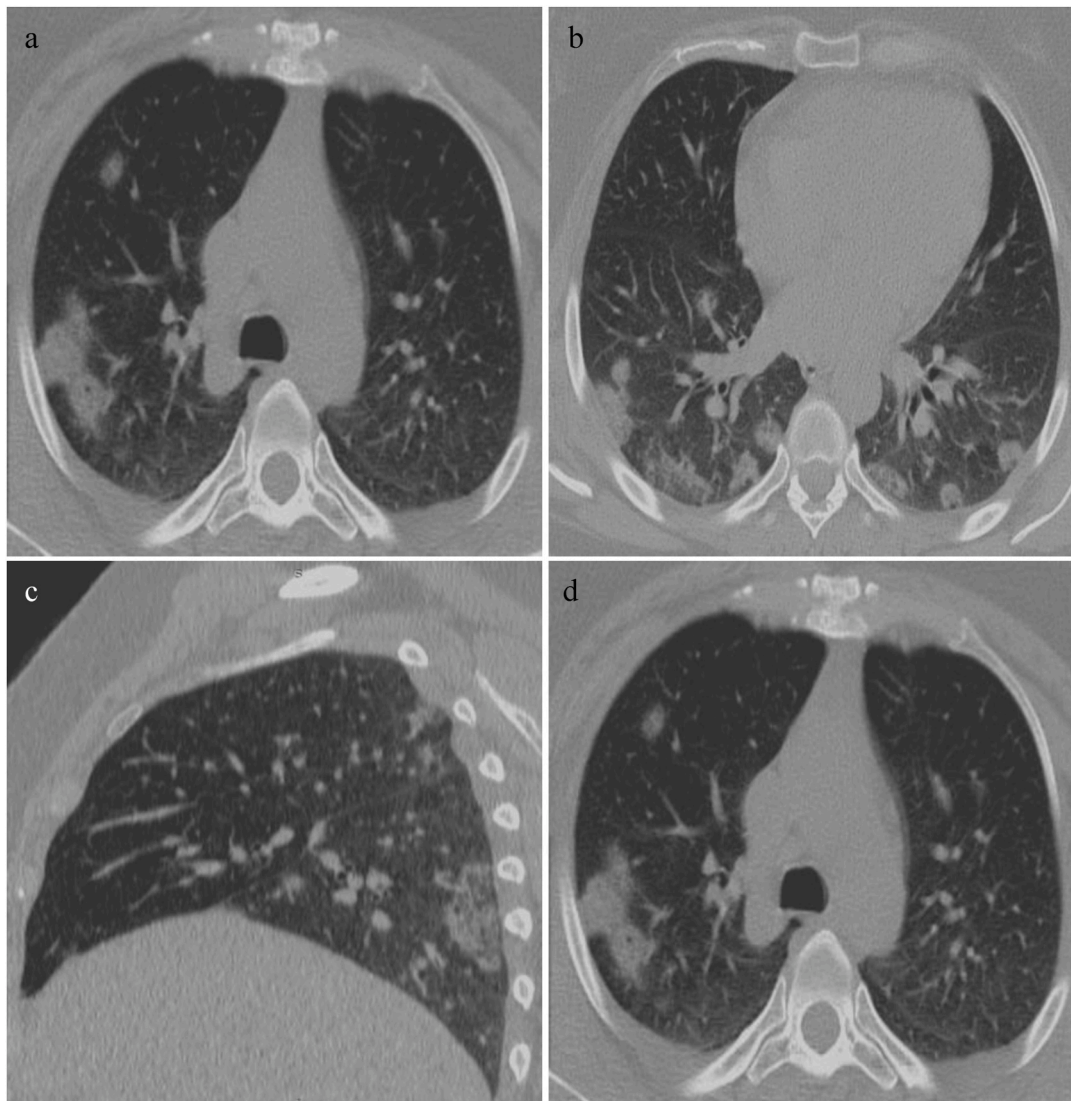


Fig. 5. Typical Covid-19 imaging features in a 45-year-old woman with a positive RT-PCR. Unenhanced axial (a, b), sagittal (c) and coronal (d) CT images of the lung show multifocal, bilateral, posterior and peripheral rounded consolidations surrounded by ground glass opacities.

3.4. Reporting templates

Current literature and expert consensus suggest standardized CT reporting templates use within the Covid-19 pneumonia context [79]. The goal is to guide radiologists, decrease reports inconsistencies and better clinicians' comprehension of radiologic features for a finer incorporation of imaging into decisions' adoption. The precise probability of Covid-19 pneumonia is not given. Four reporting categories are proposed based on the findings' typicality of Covid-19 pneumonia aspects as indicated in the literature [79].

"Typical appearance" findings are those commonly pointed out in the literature as most specific of Covid-19 pneumonia (bilateral, peripheral, multifocal, round ground glass attenuations associated or not with consolidative opacities, crazy-paving, reserve halo sign or other organized pneumonia features). The main differential diagnosis is Influenza pneumonia and organized pneumonia (connectivities, drug toxicity ...) (Figs. 5 and 6).

"Indeterminate appearance" findings are nonspecific of Covid-19 pneumonia - extensive or small ground glass attenuations lacking a specific peripheral disposition and a circular shape -, hard to differentiate radiologically from many pathologies (alveolar hemorrhage, Pneumocystis pneumonia ...) (Fig. 7).

"Atypical appearance" findings are not or infrequently reported in the setting of Covid-19 pneumonia such as tree-in-bud or centrilobular nodules, sole lobar or segmental consolidative opacities, cavities ... Bacterial pneumonia is one of the alternative diagnosis (Fig. 8).

"Negative for pneumonia" indicates the absence of infection related lung anomalies.

Of note, Covid-19 early stage CTs might be normal [79]. Describing accompanying underlying lung disease is important. Mixed typical and atypical imaging patterns coexistence (secondary infection, aspiration ...), as well as incidental findings of Covid-19 pneumonia complicate grouping and mandate direct communication with the referring physicians [80].

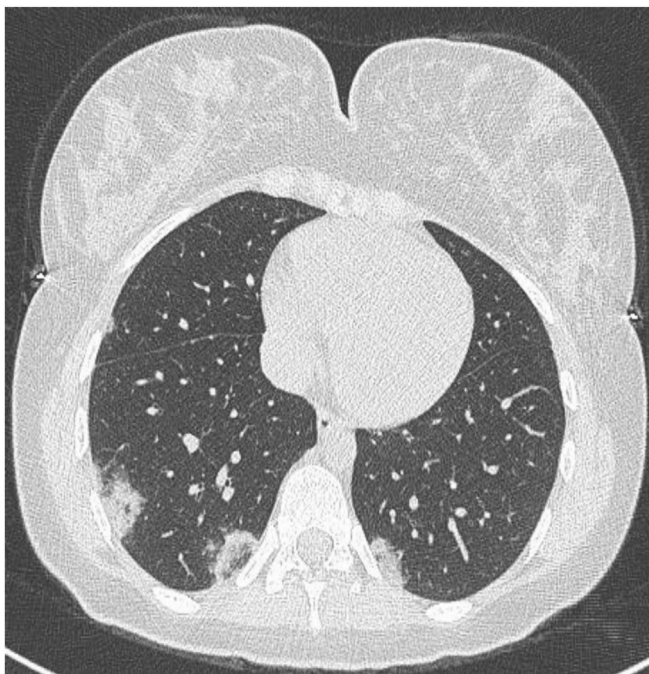


Fig. 6. Axial CT image showing bilateral posterior, peripheral, and rounded ground glass opacities in a patient with organizing pneumonia secondary to dermatomyositis; typical Covid-19 imaging features.

4. Chest radiography

Chest radiography's sensitivity for covid-19 pneumonia is limited for it fails to detect ground glass opacities; the infection's major manifestation [81]. In early disease phases, x-rays have little diagnostic input whilst CT features might precede symptoms onset [33,82]. In advanced disease, radiographs might exhibit progression towards acute respiratory distress syndrome [4]. Guan et al. reported a higher propensity of radiographic anomalies in severe disease (76.7% (46/60 patients with grave infection) versus 54.2% (116/214 cases with mild infection) [65] (Fig. 9). According to the British Society of Thoracic Imaging, when a chest radiography indicates an alternate diagnosis (lobar pneumonia, pneumothorax ...) CT offers no extra value over clinical and laboratory evaluation [12]. Chest x-rays can be of use in hospitalized patients follow-up and complications assessment [83]. Standard day-to-day chest x-rays regiments for stable mechanically ventilated covid-19 patients are not indicated; as studies comparing daily to on-demand intensive care units patients imaging revealed no significant differences in mortality, length of stay nor mechanical ventilation days [8,84,85]. Material movability might favor radiograph's use in singled populations [8].

5. Lung ultrasound

Quick, available, inexpensive, fast to disinfect and non-invasive; ultrasound uses no ionizing radiations and is portable limiting highly contagious and possibly unstable SARS-Cov2 patients transfers, at the expense of operators' exposure [86]. Current data does not support lung ultrasound's use for Covid-19' pneumonia diagnosis [87]. Although highly sensitive, ultrasonography exhibits no specific covid-19 features [87]. Reported findings comprise: pleural thickening, multifocal/coalescent B lines and consolidations; depending on the infection's phase and gravity [88]. A lines re-appearance is a recovery indicator [88]. Pleural effusion is unusual [88]. Its presence may prompt alternative diagnosis appraisal (heart failure, bacterial pneumonia ...) [89]. Deep lesions with no extension to the pleural surface cannot be detected by lung ultrasonography [88]. Its utilization in intensive care units and at point of care allows distinction between various hypoxia causes (consolidation, interstitial syndrome, pulmonary edema, pleural effusion ...), with a diagnostic accuracy superior to chest radiography permitting proper treatment's administration [89-91]. Other lung ultrasound applications include: Sars-Cov2 pneumonia severity and evolution assessment using the Lung Ultra-Sound Score potentially [92,93], directing mechanical ventilation techniques delivery (recruitment maneuvers, prone positioning, weaning ...) and guiding extracorporeal membrane oxygenation therapy [88,93].

6. MRI

The American College of Radiology advocates minimizing MRI's utilization in suspected or confirmed SARS-CoV-2 patients [94]. A major limitation to MRI's use in COVID-19 pneumonia setting is imaging equipment disinfection challenges [95]. Due to cardiac and respiratory motion artifacts, pulmonary parenchyma low proton density, and air-soft-tissue interfaces induced susceptibility artifacts, pulmonary MRI indications have been traditionally limited [96]. Nonetheless, alveolar spaces pathology-namely GGOs and consolidations -appear hyperintense in comparison to enviroing tissues due to fluid accumulation and higher proton density [97]. In radiation at-risk groups such as children and pregnant females, chest MRI is a viable imaging alternative [96]. Yang et al. ultrashort echo time MRI (UTE-MRI) showed high concordance with CT in detecting Covid-19 pneumonia typical imaging features (GGOs, consolidations, GGOs with consolidation) [98]. In Ates et al.'s study, MRI had 91.7% sensitivity, 100% specificity, 100% positive predictive value, 95.2% negative predictive value, and demonstrated no significant differences in detecting GGOs or consolidations compared to CT [97]. Multiple MRI sequences detected GGOs,

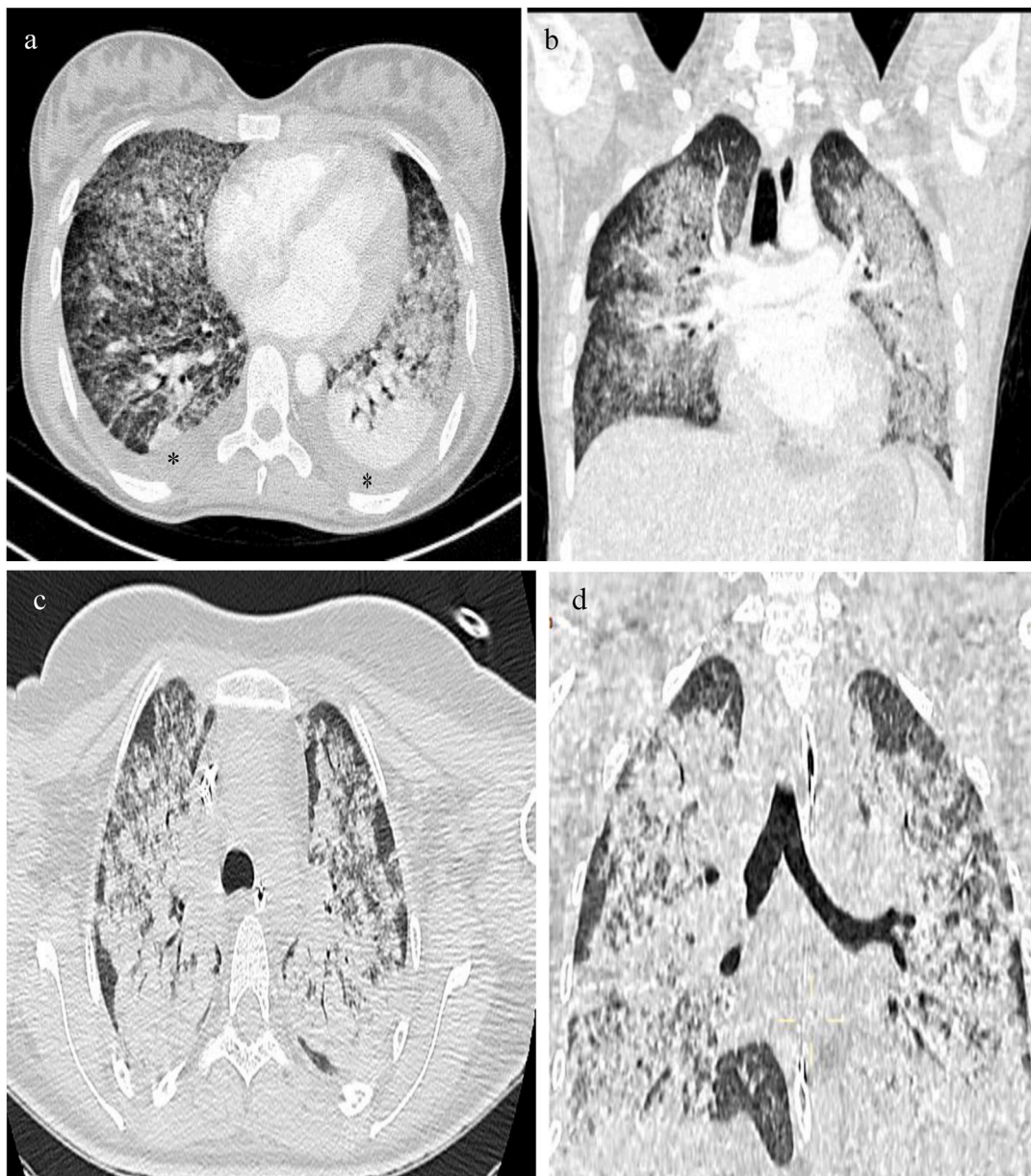


Fig. 7. ‘Indeterminate Covid-19 appearance’ Chest CT images in 2 patients showing ground glass opacities and consolidations with no specific distribution nor morphology in a case of.

(a,b) Acute eosinophilic pneumonia associating interlobular septal thickening, lower lobes air space consolidations and pleural effusions ().
(c,d) Extensive, multifocal, bilateral consolidation in a case of diffuse alveolar hemorrhage.*

consolidation, reticulation, and reverse halo sign in a case series of eight patients by Torkian et al. [99]. Among studied sequences, T2-weighted turbo spin-echo turbo inversion recovery magnitude (T2W TSE-TIRM) resolved lesions more brightly [99].

7. PET CT

While considerably sensitive, PET imaging’s applicability as a first-line Covid-19 pneumonia diagnostic modality is limited due to its low specificity, high cost, radiation risk, lengthy staff exposure, and long scanner bays disinfection and suites’ ventilation processes [100,101].

Early SARS-CoV-2 infection’s detection in asymptomatic individuals, especially vulnerable populations (immunocompromised and oncology patients) allows timely supportive care initiation, which is critical to better outcome and improve survival. In patients requiring 18-F-FDG

PET/CT for unrelated clinical indications (malignancy evaluation and staging), several reports demonstrated incidental hypermetabolic pulmonary foci in anatomic regions corresponding to Covid-19 related parenchymal abnormalities [101,102]. Jointly with PET imaging, a low-dose CT is performed, serves as a diagnostic tool, and might detect precocious pulmonary lesions justifying confirmative biological analyses [103]. In a case series of four patients who underwent 18 F-FDG PET/CT in the course of acute Covid-19 pneumonia, Qin et al. outlined parenchymal 18 F-FDG uptake in ground-glass and/or consolidative opacities regions with maximum standardized uptake (SUVmax) values varying from 4.6 to 12.2 [104]. Three patients presented nodal involvement. It was proposed that higher 18 F-FDG uptake could correlate with greater erythrocyte sedimentation rates and require more time to resolve [104–106]. In a systematic review including 52 patients, the mean SUV max of pulmonary lesions with 18 F-fluorodeoxyglucose

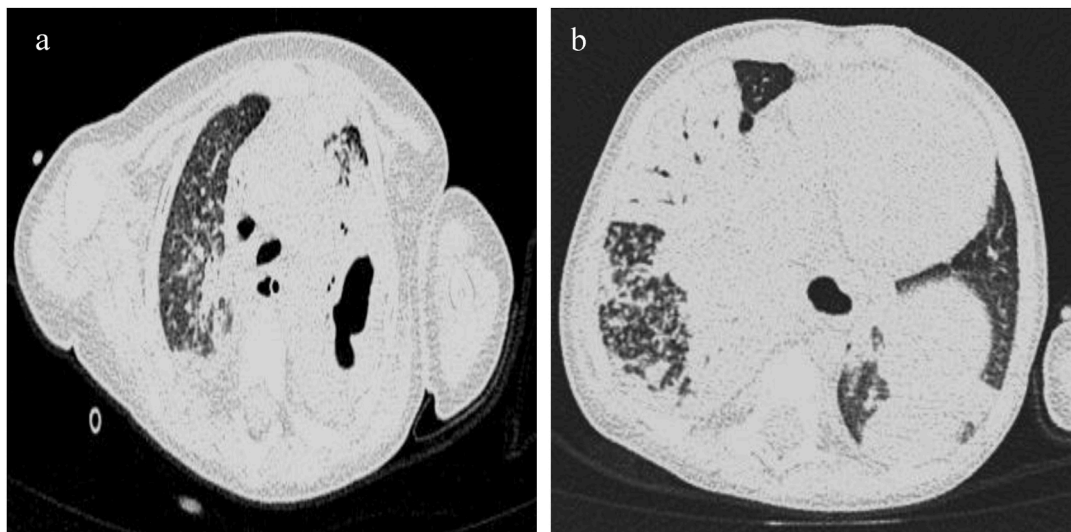


Fig. 8. Atypical Covid-19 C T features. Unenhanced axial chest CT images showing segmental consolidations with no ground glass opacities, cavitation alongside with centrilobular and tree-in-bud nodules in an active tuberculous infection (a,b).



Fig. 9. Frontal chest radiography showing bilateral air space consolidations in a Covid-19 patient.

uptake was 4.9 ± 2.3 [107]. ^{18}F -FDG PET/CT could be of use in evaluating other organs' alterations, particularly the heart, kidneys, and digestive tract [106]. Two patients undergoing PET/CT for prostate cancer showed ^{68}Ga -labelled prostate-specific membrane antigen (^{68}Ga -PSMA) and ^{18}F -labelled choline (^{18}F -choline) uptake in subpleural GGO regions [108].

8. Artificial intelligence imaging applications

In the fight against Covid-19, artificial intelligence empowered imaging might strengthen available tools and help radiologists [109]. Scanning's automation relying on shifting CT tables and visual sensors enables contact-free imaging. Lung lobes and lesions segmentation is applied in Covid-19 diagnosis and quantification [109].

Artificial intelligence can assist both chest x-ray and CT Covid-19 screening, differential diagnosis and severity assessment.

In a study including x-rays of 70 covid-19 patients and 1008 non covid-19 pneumonias, Zhang et al. introduced a ResNet model to discern radiographic Covid-19 findings. Sensitivity and specificity were 96.0% and 70.7% with an AUC of 0.952 [110].

Similarly, Wang et al. applied a deep convolutional neural network founded model to identify Covid-19 radiographic features among chest x-rays images of 931 bacterial pneumonias, 45 Covid-19 pneumonias, 660 viral pneumonias and 1203 normal cases. The obtained testing accuracy was of 83.5% [111].

Chen et al. reported that with artificial intelligence performances aid; radiologists' chest CT reading time is reduced by 65% [112].

To train and test a deep learning model for Covid-19 diagnosis; Zheng et al. used 540 chest CTs (313 covid-19 positives and 229 covid-19 negatives). Achieved sensitivity and specificity were 90.7% and 91.1% respectively, with an AUC of 0.959 [113].

In a similar manner, Jin et al. used a UNet and ResNet 50 combined model for abnormalities localization and diagnosis. Their study included 1136 chest CTs (723 with Covid-19 and 413 without covid-19 pneumonia). The sensitivity and specificity were 97.4% and 92.2% respectively [114].

To distinguish Covid-19 from typical viral pneumonia, Xu et al. testing dataset included chest CT images from 219 Covid-19 patients, 224 Influenza-A cases and 175 healthy subjects. Their model's overall accuracy was of 86.7% [115].

Likewise, Li et al. used a significant dataset comprising 4356 chest computed tomography images from 1296 Covid-19 pneumonias, 1735 community-acquired pneumonias and 1325 cases with no pneumonia. Their model's achieved sensitivity in depicting covid-19 was 90%, specificity 96% and AUC 0.96 [116].

To assess Covid-19 pneumonia's severity (severe or not), Tang et al. endorsed a deep learning method to segment the pulmonary parenchyma into anatomical regions [117]; on the basis of which, infection ratios were measured and employed as quantitative traits to instruct the model that analyzed chest CTs of 176 Covid-19 confirmed cases. A true positive rate of 93.3%, a true negative rate of 74.5% and an accuracy of 87.5% were noted [118].

In Covid-19 follow-up studies; artificial intelligence application is in its early phases and remains a pending question [109].

9. Imaging in pediatric patients

Cai et al. reported one-sided patchy infiltrates in 40% (4/10) of their covid-19 pediatric patients chest x-rays [119].

Xia et al. retrospectively analyzed chest CT features of 20 Covid-19 pediatric inpatients. Lung lesions presented a subpleural distribution. They were unilateral in 30% (6/20) and bilateral in 50% (10/20) of cases. 3 neonates and one infant had normal initial chest CTs (20%, 4/20). Ground glass attenuations were noted in 60% (12/20), Halo sign consolidation in 50% (10/20) and tiny nodules in 15% (3/20) of patients. No pleural effusion nor lymphadenopathy were reported [120].

In a review including 2597 Covid-19 pediatric patients, 409 children's chest CTs were available, among which 178 (43.5%) showed no anomalies, 2 (2/409, 0.5%) presented white lungs and 3 (3/409, 0.7%) pleural effusion [121]. Findings from 294 cases were categorized as follows: 87/294 (29.6%) patients had ground glass attenuations, 60/294 (20.4%) focal patchy shadows, 43/294 (14.6%) two-sided spotty shadows and 2/294 (0.7%) interstitial abnormalities. Chest CTs of four asymptomatic children revealed typical Covid-19 pneumonia imaging features [62]. Asymptomatic cases percentage is higher in children (7.6%) than in adults (1%) [122], highlighting the role of chest CT in early Covid-19 diagnostic work-up.

In a systematic review and meta-analysis including 9 pediatric Covid-19 case series, Chang et al. reported imaging features were analogous to those of adults [123]; the commonest being ground glass attenuations in 48% (95% CI 0.36–0.64; I2 = 5%, p = 0.52) and patchy consolidative opacities in 31% (95% CI 0.13–0.55; I2 = 51%, p = 0.09) of cases. 27% (95% CI 0.18–0.43; I2 = 0%, p = 0.64) of patients demonstrated no radiological abnormalities [124].

Covid-19 pneumonia's incidence in pediatric patients is low, clinical manifestations mild, course of disease curtailed and imaging features atypical in comparison with adults' forms potentially leading to misdiagnosis if solely depending on chest CT to screen infants. Posterior and peripheral lungs ground glass opacities appear less dense, limited in extent and may present in small nodular shapes [120,125,126]. Light forms are commoner in children and may present normal chest CTs [120,125,126]. Infrequently, disease progresses. Ground glass attenuations enlarge, increase in density, turn into multifocal consolidations and interstitial lesions become more apparent [126]. 'White lung' aspect rarely occurs [126]. In the recovery stage, complete lung abnormalities resolution takes place or merely slight linear attenuations persist [127]. Coinfections are usual in children rendering case preclusion difficult in the setting of determined epidemiological history and nonspecific CT features [120]. Numerous children exhibit pleural effusion [128]. Enlarged mediastinal lymph nodes were not reported. Scanning's indications careful weighting and low dose CT utilization are crucial to protect children from irradiation hazard. Chest CT supports diagnosis in considerably suspected patients with initially negative RT-PCR. Some RT-PCR positive children with initially normal CTs might develop anomalies subsequently. Since mild forms prevail in children, follow-up CT is only justifiable in the setting of clinical worsening and chest X-rays may represent a monitoring alternative [120,125,126]. In the absence of suggestive clinical manifestations and epidemiological history, chest radiography's usual indications are sustained (unexplained fever, abnormal pulmonary auscultation ...) [129].

10. Imaging in pregnant women

Pregnant patients with confirmed Covid-19's imaging features are comparable to those of non-pregnant adults. In a study including 23 pregnant inpatients, chest CT showed subpleural ground glass attenuations, consolidative opacities, interstitial thickening, fibrous bands as well as concomitant pleural and/or pericardial effusions [95].

Elshafeey et al. systematic review included 385 pregnant women with Covid-19 pneumonia. Chest imaging informations were accessible for 125 patients (32.5%). 4 women (3.2%) had normal chest CTs.

Bilateral anomalies were found in 99 patients (79.2%). Ground glass attenuations were noted in 81.6% (102), consolidative opacities in 17.6% (22), a reticular pattern in 0.8% (1), atelectasis in 0.8% (1), crazy paving in 0.8% (1), thickened pleura in 0.8% (1) and hydrothorax in 7.2% (9) of cases [130].

Pregnant women imaging's indications (chest x-ray and CT) should be carefully weighted to minimize irradiations' risks and patients well informed prior to their performance. Low-dose Ct scans are recommended [131], and fetus's local protection must be employed. The first trimester of pregnancy warrants special considerations for radiation's hazard. In this setting, proceeding to CT only when an initial chest x-ray is inconclusive is advisable [132].

11. Imaging of neurological manifestations

Poyiadji et al. reported the first presumed case of covid-19 related acute necrotizing hemorrhagic encephalopathy in a female patient admitted for cough, hyperthermia and mental status impairment whose nasopharyngeal swab RT-PCR was positive for Sars-CoV 2. Sars-Cov2 testing in the CSF was not performed. Brain CT demonstrated symmetrical bi-thalamic hypodensities with patent cerebral veins. Brain MRI revealed bilateral medial temporal lobes and thalami hemorrhagic lesions with ring of contrast enhancement [133].

In a correspondence to the new England journal of medicine, Helms et al. report neurologic manifestations in 58 patients admitted to Strasbourg intensive care units for covid-19 induced acute respiratory distress syndrome. 69% (40/58) were agitated, 67% (39/58) presented corticospinal tract signs and 36% (14/39) displayed a dysexecutive syndrome. Brain MRI was obtained in 13 cases and exhibited leptomeningeal enhancement in 62% (8/13), ischemic stroke in 23% (3/13) and perfusion anomalies in 100% (11/11) of patients [134].

Evidence determining whether these neurological features are specific to Sars-Cov2 infection or result from cytokine storm syndrome, severe disease-associated encephalopathy or drugs are still lacking [133, 134]. In suspected or confirmed Covid-19 patients with neurological expressions; performing Brain MRI is encouraged.

12. Limitations

Our review has some limitations. The Covid-19 pandemic being a quickly evolving situation, rapid data sharing necessity could affect released reports' quality. Despite new informations being published on a day-to-day basis rendering continual update an imperative, we think that major reported disease imaging findings will not be modified. Included studies were mainly case reports and case series limiting evidence certainty. Several reports were retrospective with a restricted sample size. Data accessibility was limited in certain instances. Larger cohorts and further longitudinal research are needed to clarify long-term follow-up outcomes and pulmonary sequelae. The correlation between imaging findings and anatomopathological pulmonary alterations are yet to be thoroughly investigated.

13. Recommendations

In asymptomatic patients, CT is not recommended as a Covid-19 screening test [79]. Nevertheless, when rapid PCR results are unavailable, chest CT can detect silent pulmonary lesions in emergency admissions with unidentified Covid-19 status whose conditions do not permit awaiting for biological tests results: urgent surgeries or therapeutic stances (stroke, bleeding). Imaging patients with mild Covid-19 symptoms is not indicated unless they have comorbidities (diabetes, chronic respiratory conditions and others more) [8,45]. In patients with moderate to severe Covid-19 features (dyspnea, desaturation) and regardless of tests results, CT is recommended to evaluate disease extent at baseline, help predict outcome and assisted ventilation requirements [45]. When initial RT-PCR tests are negative while CT findings indicate a

Covid-19 pneumonia, testing is repeated to exclude false negatives [45]. A deteriorating respiratory status warrants a repeat CT [8,45]. Pulmonary embolism suspicions prompt contrast enhanced CT performance [45]. Reiterated CTs are not indicated in patients recovering from Covid-19 with no breathing impairment nor hypoxemia [8,45]. Repeat CTs indications should be cautiously weighted as Sars-Cov2 infected patients transportation from wards to radiology departments yields a high risk of contaminating other patients and health care workers [45]. Using standardized Covid-19 C T reporting language is recommended [79]. Chest radiography and lung ultrasound should not be used as a first-line screening or diagnostic test. Chest x-rays are used for non-transportable intensive-care-units patients follow-up while ultrasound is a bed-side tool that allows assisted ventilation parameters adjustment, induced complications diagnosis and fluid load surveillance [45].

14. Conclusion

In conclusion, this review offers an exhaustive analysis of the current literature on imaging role and findings in COVID-19 pneumonia. Chest CT plays an invaluable part notably in early disease detection in cases of high clinical suspicion and negative or inaccessible RT-PCR as well as pneumonia progression and treatment response evaluation. Guidelines and reporting templates provide a framework for radiologists to follow and better communication with clinicians. As this pandemic continues its rapid surge; artificial intelligence mediated imaging could strengthen available tools and help radiology staff.

Ethical Approval

Ethical approval was not required.

Consent

Consent for publication was not applicable.

Author contribution

Hanae Ramdani and Nazik Allali: Contributed to conception, acquisition, analysis, and interpretation of data; drafted the manuscript. Siham el Haddad and Latifa Chat: Critically revised manuscript. All the authors have read and approved the final draft of the manuscript.

Registration of Research Studies

1. Name of the registry:
2. Unique Identifying number or registration ID:
3. Hyperlink to your specific registration (must be publicly accessible and will be checked):

Guarantor

Hanae Ramdani.
Email address: hanaeramdani@hotmail.fr.

Consent for publication

Not applicable.

Declaration of competing interest

Authors have no conflicts of interest.
No funding was received.

Acknowledgements

All authors contributed substantially to the design and reporting of this manuscript. We appreciate the input from Dr Y.Mellagui and Dr S. Nasri who helped with the imaging data acquisition.

References

- [1] Y. Cao, X. Liu, L. Xiong, K. Cai, Imaging and clinical features of patients with 2019 novel coronavirus SARS-CoV-2: a systematic review and meta-analysis, *J. Med. Virol.* 92 (9) (2020 Sep) 1449–1459.
- [2] L.J. Borges do Nascimento, N. Cacic, H.M. Abdulazeem, et al., Novel coronavirus infection (COVID-19) in humans: a scoping review and meta-analysis, *J. Clin. Med.* 9 (4) (2020 Apr) 941.
- [3] A.J. Rodriguez-Morales, J.A. Cardona-Ospina, E. Gutiérrez-Ocampo, et al., Clinical, laboratory and imaging features of COVID-19: a systematic review and meta-analysis, *Trav. Med. Infect. Dis.* 34 (2020 Mar 1) 101623.
- [4] S. Salehi, A. Abedi, S. Balakrishnan, A. Gholamrezanezhad, Coronavirus disease 2019 (COVID-19): a systematic review of imaging findings in 919 patients, *Am. J. Roentgenol.* 215 (1) (2020 Jul) 87–93.
- [5] J. Liu, H. Yu, S. Zhang, The indispensable role of chest CT in the detection of coronavirus disease 2019 (COVID-19), *Eur. J. Nucl. Med. Mol. Imag.* 47 (7) (2020 Jul) 1638–1639.
- [6] M. Chung, A. Bernheim, X. Mei, et al., CT imaging features of 2019 novel coronavirus (2019-nCoV), *Radiology* 295 (1) (2020 Apr) 202–207.
- [7] S. Kooraki, M. Hosseiny, L. Myers, A. Gholamrezanezhad, Coronavirus (COVID-19) outbreak: what the department of radiology should know, *J. Am. Coll. Radiol.* 17 (4) (2020 Apr 1) 447–451.
- [8] G.D. Rubin, C.J. Ryerson, L.B. Haramati, et al., The role of chest imaging in patient management during the COVID-19 pandemic: a multinational consensus statement from the Fleischner Society, *Chest* 158 (1) (2020 Jul 1) 106–116.
- [9] N. Sverzellati, F. Milone, M. Balbi, How imaging should properly be used in COVID-19 outbreak: an Italian experience, *Diagn. Intervent. Radiol.* 26 (3) (2020 May) 204.
- [10] J. Czernin, S. Fanti, P.T. Meyer, et al., Nuclear medicine operations in the times of COVID-19: strategies, precautions, and experiences, *J. Nucl. Med.* 61 (5) (2020 May 1) 626–629.
- [11] N. Sverzellati, G. Milanese, F. Milone, M. Balbi, R.E. Ledda, M. Silva, Integrated radiologic algorithm for COVID-19 pandemic, *J. Thorac. Imag.* 35 (4) (2020 Jul 1) 228–233.
- [12] A. Nair, J.C. Rodrigues, S. Hare, et al., A British Society of Thoracic Imaging statement: considerations in designing local imaging diagnostic algorithms for the COVID-19 pandemic, *Clin. Radiol.* 75 (5) (2020 May 1) 329–334.
- [13] Centers for Disease Control and Prevention, Interim Guidelines for Collecting, Handling, and Testing Clinical Specimens from Persons under Investigation (PUIs) for Coronavirus Disease 2019 (COVID-19). COVID-19, 2020. Mar 9.
- [14] X. Xie, Z. Zhong, W. Zhao, C. Zheng, F. Wang, J. Liu, Chest CT for typical coronavirus disease 2019 (COVID-19) pneumonia: relationship to negative RT-PCR testing, *Radiology* 296 (2) (2020 Aug) E41–E45.
- [15] Y. Fang, H. Zhang, J. Xie, et al., Sensitivity of chest CT for COVID-19: comparison to RT-PCR, *Radiology* 296 (2) (2020 Aug) E115–E117.
- [16] J. Xu, R. Wu, H. Huang, et al., Computed tomographic imaging of 3 patients with coronavirus disease 2019 pneumonia with negative virus real-time reverse-transcription polymerase chain reaction test, *Clin. Infect. Dis.* 71 (15) (2020 Jul 28) 850–852.
- [17] D.K. Chu, Y. Pan, S.M. Cheng, et al., Molecular diagnosis of a novel coronavirus (2019-nCoV) causing an outbreak of pneumonia, *Clin. Chem.* 66 (4) (2020 Apr 1) 549–555.
- [18] D. Li, D. Wang, J. Dong, et al., False-negative results of real-time reverse-transcriptase polymerase chain reaction for severe acute respiratory syndrome coronavirus 2: role of deep-learning-based CT diagnosis and insights from two cases, *Korean J. Radiol.* 21 (4) (2020 Apr) 505.
- [19] W.C. Dai, H.W. Zhang, J. Yu, et al., CT imaging and differential diagnosis of COVID-19, *Can. Assoc. Radiol. J.* 71 (2) (2020 May) 195–200.
- [20] X. Xie, Z.W. Zhong, C. Zheng, F. Wang, J. Liu, Chest CT for typical 2019-nCoV pneumonia: relationship to negative RT-PCR testing, *Radiology* (2020) 200343.
- [21] H. Dai, X. Zhang, J. Xia, et al., High-resolution chest CT features and clinical characteristics of patients infected with COVID-19 in Jiangsu, China, *Int. J. Infect. Dis.* 95 (2020 Jun 1) 106–112.
- [22] J.P. Kanne, B.P. Little, J.H. Chung, B.M. Elicker, L.H. Ketaj, Essentials for Radiologists on COVID-19: an Update—Radiology Scientific Expert Panel, *Radiol.* 296 (2) (2020 August) E113–E114.
- [23] Y. Wan, J. Shang, R. Graham, R.S. Baric, F. Li, Receptor recognition by the novel coronavirus from Wuhan: an analysis based on decade-long structural studies of SARS coronavirus, *J. Virol.* (7) (2020 Mar 17) 94.
- [24] Y. Wang, C. Dong, Y. Hu, et al., Temporal changes of CT findings in 90 patients with COVID-19 pneumonia: a longitudinal study, *Radiology* 296 (2) (2020 Aug) E55–E64.
- [25] X. Li, W. Zeng, X. Li, et al., CT imaging changes of corona virus disease 2019 (COVID-19): a multi-center study in Southwest China, *J. Transl. Med.* 18 (2020 Dec) 1–8.
- [26] C.S. Guan, Z.B. Lv, S. Yan, et al., Imaging features of coronavirus disease 2019 (COVID-19): evaluation on thin-section CT, *Acad. Radiol.* 27 (5) (2020 May 1) 609–613.

- [27] N. Chen, M. Zhou, X. Dong, et al., Epidemiological and clinical characteristics of 99 cases of 2019 novel coronavirus pneumonia in Wuhan, China: a descriptive study, *Lancet* 395 (10223) (2020 Feb 15) 507–513.
- [28] B.M. Elicker, B.S. Schwartz, C. Liu, et al., Thoracic CT findings of novel influenza A (H1N1) infection in immunocompromised patients, *Emerg. Radiol.* 17 (4) (2010 Jul) 299–307.
- [29] L. Gao, J. Zhang, Pulmonary high-resolution computed tomography (HRCT) findings of patients with early-stage coronavirus disease 2019 (COVID-19) in Hangzhou, China, *Med. Sci. Mon. Int. Med. J. Exp. Clin. Res.* 26 (2020) e923885-1.
- [30] M. Yuan, W. Yin, Z. Tao, W. Tan, Y. Hu, Association of radiologic findings with mortality of patients infected with 2019 novel coronavirus in Wuhan, China, *PLoS One* 15 (3) (2020 Mar 19), e0230548.
- [31] C. Long, H. Xu, Q. Shen, et al., Diagnosis of the Coronavirus disease (COVID-19): rRT-PCR or CT? *Eur. J. Radiol.* 126 (2020 May 1) 108961.
- [32] Y.H. Jin, L. Cai, Z.S. Cheng, et al., A rapid advice guideline for the diagnosis and treatment of 2019 novel coronavirus (2019-nCoV) infected pneumonia (standard version), *Military Medical Research* 7 (1) (2020 Dec) 1–23.
- [33] Y. Pan, H. Guan, S. Zhou, et al., Initial CT findings and temporal changes in patients with the novel coronavirus pneumonia (2019-nCoV): a study of 63 patients in Wuhan, China, *Eur. Radiol.* 30 (6) (2020 Jun) 3306–3309.
- [34] F. Pan, T. Ye, P. Sun, et al., Time course of lung changes on chest CT during recovery from 2019 novel coronavirus (COVID-19) pneumonia, *Radiology* 295 (3) (2020 Feb 13) 715–721.
- [35] H. Shi, X. Han, N. Jiang, et al., Radiological findings from 81 patients with COVID-19 pneumonia in Wuhan, China: a descriptive study, *Lancet Infect. Dis.* 20 (4) (2020 Apr 1) 425–434.
- [36] C. Huang, Y. Wang, X. Li, et al., Clinical features of patients infected with 2019 novel coronavirus in Wuhan, China, *Lancet* 395 (10223) (2020 Feb 15) 497–506.
- [37] L. Ketai, N.S. Paul, T.W. Ka-tak, Radiology of severe acute respiratory syndrome (SARS): the emerging pathologic-radiologic correlates of an emerging disease, *J. Thorac. Imag.* 21 (4) (2006 Nov 1) 276–283.
- [38] S. Chong, T.S. Kim, E.Y. Cho, Herpes simplex virus pneumonia: high-resolution CT findings, *BJR (Br. J. Radiol.)* 83 (991) (2010 Jul) 585–589.
- [39] D.M. Hansell, A.A. Bankier, H. MacMahon, T.C. McLoud, N.L. Muller, J. Remy, Fleischner Society: glossary of terms for thoracic imaging, *Radiology* 246 (3) (2008 Mar) 697–722.
- [40] Z.W. Lang, L.J. Zhang, S.J. Zhang, et al., A clinicopathological study on 3 cases of severe acute respiratory syndrome, *Zhonghua bing li xue za zhi = Chinese journal of pathology* 32 (3) (2003 Jun 1) 201–204.
- [41] J.M. Nicholls, L.L. Poon, K.C. Lee, et al., Lung pathology of fatal severe acute respiratory syndrome, *Lancet* 361 (9371) (2003 May 24) 1773–1778.
- [42] Y. Ding, H. Wang, H. Shen, et al., The clinical pathology of severe acute respiratory syndrome (SARS): a report from China, *J. Pathol.: A J Pathological Soc Great Britain and Ireland* 200 (3) (2003 Jul) 282–289.
- [43] L. Grinblat, H. Shulman, A. Glickman, L. Matukas, N. Paul, Severe acute respiratory syndrome: radiographic review of 40 probable cases in Toronto, Canada, *Radiology* 228 (3) (2003 Sep) 802–809.
- [44] Q. Wang, Z. Zhang, Y. Shi, Y. Jiang, Emerging H7N9 influenza A (novel reassortant avian-origin) pneumonia: radiologic findings, *Radiology* 268 (3) (2013 Sep) 882–889.
- [45] M.P. Revel, A.P. Parkar, H. Prosch, et al., COVID-19 patients and the radiology department—advice from the European society of radiology (ESR) and the European society of thoracic imaging (ESTI), *Eur. Radiol.* 30 (9) (2020 Sep) 4903–4909.
- [46] A. Zarifian, M.G. Nour, A.A. Rezayat, R.R. Oskooei, B. Abbasi, R. Sadeghi, Chest CT findings of coronavirus disease 2019 (COVID-19): a comprehensive meta-analysis of 9907 confirmed patients, *Clin. Imag.* 70 (2021 Feb 1) 101–110.
- [47] Z. Sun, N. Zhang, Y. Li, X. Xu, A systematic review of chest imaging findings in COVID-19. Quantitative imaging in medicine and surgery 10 (5) (2020 May) 1058.
- [48] T.H. Chang, J.L. Wu, L.Y. Chang, Clinical characteristics and diagnostic challenges of pediatric COVID-19: a systematic review and meta-analysis, *J. Formos. Med. Assoc.* 119 (5) (2020 May 1) 982–989.
- [49] F. Elshafeey, R. Magdi, N. Hindi, et al., A systematic scoping review of COVID-19 during pregnancy and childbirth, *Int. J. Gynecol. Obstet.* 150 (1) (2020 Jul) 47–52.
- [50] J. Kumar, J. Meena, A. Yadav, J. Yadav, Radiological findings of COVID-19 in children: a systematic review and meta-analysis, *J. Trop. Pediatr.* (2020 Jul 21).
- [51] X. Cui, T. Zhang, J. Zheng, et al., Children with coronavirus disease 2019: a review of demographic, clinical, laboratory, and imaging features in pediatric patients, *J. Med. Virol.* 92 (9) (2020 Sep) 1501–1510.
- [52] S. Wan, M. Li, Z. Ye, C. Yang, Q. Cai, S. Duan, B. Song, CT manifestations and clinical characteristics of 1115 patients with coronavirus disease 2019 (COVID-19): a systematic review and meta-analysis, *Acad. Radiol.* 27 (7) (2020 Jul 1) 910–921.
- [53] E. Awulachew, K. Diriba, A. Anja, E. Getu, F. Belayneh, Computed tomography (CT) imaging features of patients with COVID-19: systematic review and meta-analysis, *Radiology Research and Practice* (2020 Jul 23) 2020.
- [54] C.R. Jutzeler, L. Bourguignon, C.V. Weis, et al., Comorbidities, clinical signs and symptoms, laboratory findings, imaging features, treatment strategies, and outcomes in adult and pediatric patients with COVID-19: a systematic review and meta-analysis, *Trav. Med. Infect. Dis.* (2020 Aug 4) 101825.
- [55] M.F. Mohamed, S. Al-Shokri, Z. Yousof, et al., Frequency of abnormalities detected by point-of-care lung ultrasound in symptomatic COVID-19 patients: systematic review and meta-analysis, *Am. J. Trop. Med. Hyg.* 103 (2) (2020 Aug 5) 815–821.
- [56] S.Z. Muhammad, A. Ahmed, I. Shahid, et al., Chest computed tomography findings in hospitalized COVID-19 patients: a systematic review and meta-analysis, *Inf. Med.* 28 (2020 Sep 1) 295–301.
- [57] B. Xu, Y. Xing, J. Peng, et al., Chest CT for detecting COVID-19: a systematic review and meta-analysis of diagnostic accuracy, *Eur. Radiol.* 30 (2020 Oct) 5720.
- [58] Y. Choi, M.K. Lee, Neuroimaging findings of brain MRI and CT in patients with COVID-19: a systematic review and meta-analysis, *Eur. J. Radiol.* (2020 Nov 3) 109393.
- [59] M. Garg, P. Gupta, M. Maralakunte, -M.P. Kumar, et al., Diagnostic accuracy of CT and radiographic findings for novel coronavirus 2019 pneumonia: systematic review and meta-analysis, *Clin. Imag.* 72 (2020 Nov 11) 75–82.
- [60] M. Islam, T.N. Poly, B.A. Walther, et al., Clinical characteristics and neonatal outcomes of pregnant patients with COVID-19: a systematic review, *Front. Med.* 7 (2020) 909.
- [61] G. Nino, J. Zember, R. Sanchez-Jacob, M.J. Gutierrez, K. Sharma, M.G. Linguraru, Pediatric lung imaging features of COVID-19: a systematic review and meta-analysis, *Pediatr. Pulmonol.* 56 (1) (2021 Jan) 252–263.
- [62] J.F. Chan, S. Yuan, K.H. Kok, et al., A familial cluster of pneumonia associated with the 2019 novel coronavirus indicating person-to-person transmission: a study of a family cluster, *Lancet* 395 (10223) (2020 Feb 15) 514–523.
- [63] F. Song, N. Shi, F. Shan, et al., Emerging 2019 novel coronavirus (2019-nCoV) pneumonia, *Radiology* 295 (1) (2020 Apr) 210–217.
- [64] J.R. Flowers, G. Clunie, M. Burke, O. Constant, Bronchiolitis obliterans organizing pneumonia: the clinical and radiological features of seven cases and a review of the literature, *Clin. Radiol.* 45 (6) (1992 Jun 1) 371–377.
- [65] W.J. Guan, Z.Y. Ni, Y. Hu, et al., Clinical characteristics of coronavirus disease 2019 in China, *N. Engl. J. Med.* 382 (18) (2020 Apr 30) 1708–1720.
- [66] H.X. Bai, B. Hsieh, Z. Xiong, et al., Performance of radiologists in differentiating COVID-19 from non-COVID-19 viral pneumonia at chest CT, *Radiology* 296 (2) (2020 Aug) E46–E54.
- [67] V.M. Corman, O. Landt, M. Kaiser, et al., Detection of 2019 novel coronavirus (2019-nCoV) by real-time RT-PCR, *Euro Surveill.* 25 (3) (2020 Jan 23) 2000045.
- [68] T. Kishaba, Community-acquired pneumonia caused by *Mycoplasma pneumoniae*: how physical and radiological examination contribute to successful diagnosis, *Front. Med.* 3 (2016 Jun 13) 28.
- [69] K.T. Wong, G.E. Antonio, D.S. Hui, et al., Severe acute respiratory syndrome: radiographic appearances and pattern of progression in 138 patients, *Radiology* 228 (2) (2003 Aug) 401–406.
- [70] K.M. Das, E.Y. Lee, R.D. Langer, S.G. Larsson, Middle East respiratory syndrome coronavirus: what does a radiologist need to know? *Am. J. Roentgenol.* 206 (6) (2016 Jun) 1193–1201.
- [71] W.J. Choi, K.N. Lee, E.J. Kang, H. Lee, Middle East respiratory syndrome-coronavirus infection: a case report of serial computed tomographic findings in a young male patient, *Korean J. Radiol.* 17 (1) (2016 Jan) 166.
- [72] G.C. Ooi, P.L. Khong, N.L. Müller, et al., Severe acute respiratory syndrome: temporal lung changes at thin-section CT in 30 patients, *Radiology* 230 (3) (2004 Mar) 836–844.
- [73] N.L. Müller, G.C. Ooi, P.L. Khong, L.J. Zhou, K.W. Tsang, S. Nicolaou, High-resolution CT findings of severe acute respiratory syndrome at presentation and after admission, *Am. J. Roentgenol.* 182 (1) (2004 Jan) 39–44.
- [74] J.S. Peiris, C.M. Chu, V.C. Cheng, et al., Clinical progression and viral load in a community outbreak of coronavirus-associated SARS pneumonia: a prospective study, *Lancet* 361 (9371) (2003 May 24) 1767–1772.
- [75] K.M. Das, E.Y. Lee, S.E. Jawder, et al., Acute Middle East respiratory syndrome coronavirus: temporal lung changes observed on the chest radiographs of 55 patients, *Am. J. Roentgenol.* 205 (3) (2015 Sep) W267–S274.
- [76] K.M. Das, E.Y. Lee, M.A. Enani, et al., CT correlation with outcomes in 15 patients with acute Middle East respiratory syndrome coronavirus, *Am. J. Roentgenol.* 204 (4) (2015 Apr) 736–742.
- [77] D. Wang, C. Wu, J. Gao, et al., Comparative study of primary pulmonary cryptococcosis with multiple nodules or masses by CT and pathology, *Experimental and therapeutic medicine* 16 (6) (2018 Dec 1) 4437–4444.
- [78] H. Lu, C.W. Stratton, Y.W. Tang, Outbreak of pneumonia of unknown etiology in Wuhan, China: the mystery and the miracle, *J. Med. Virol.* 92 (4) (2020 Apr) 401–402.
- [79] S. Simpson, F.U. Kay, S. Abbara, et al., Radiological society of north America expert consensus document on reporting chest CT findings related to COVID-19: endorsed by the society of thoracic Radiology, the American college of Radiology, and RSNA. *Radiology: cardiothoracic Imaging* 2 (2) (2020 Mar 25), e200152.
- [80] N. Shah, I. Brown, Higher co-infection rates in COVID19, *Medium. Com* (2020 April).
- [81] S.H. Yoon, K.H. Lee, J.Y. Kim, et al., Chest radiographic and CT findings of the 2019 novel coronavirus disease (COVID-19): analysis of nine patients treated in Korea, *Korean J. Radiol.* 21 (4) (2020 Apr) 494.
- [82] J.Y. Kim, P.G. Choe, Y. Oh, et al., The first case of 2019 novel coronavirus pneumonia imported into Korea from Wuhan, China: implication for infection prevention and control measures, *J. Kor. Med. Sci.* 35 (5) (2020 Feb 10).
- [83] J.R. Hill, P.E. Horner, S.L. Primack, ICU imaging, *Clin. Chest Med.* 29 (1) (2008 Mar 1) 59–76.
- [84] Y. Oba, T. Zaza, Abandoning daily routine chest radiography in the intensive care unit: meta-analysis, *Radiology* 255 (2) (2010 May) 386–395.
- [85] R.D. Suh, S.J. Genshaft, J. Kirsch, et al., ACR Appropriateness Criteria® intensive care unit patients, *J. Thorac. Imag.* 30 (6) (2015 Nov 1) W63–W65.

- [86] P.H. Mayo, R. Copetti, D. Feller-Kopman, et al., Thoracic ultrasonography: a narrative review, *Intensive Care Med.* 45 (9) (2019 Sep) 1200–1211.
- [87] S. Moore, E. Gardiner, Point of Care and Intensive Care Lung Ultrasound: A Reference Guide for Practitioners during COVID-19, *Radiography* 26 (4) (2020 Apr 17) 297–302.
- [88] Q.Y. Peng, X.T. Wang, L.N.G. Zhang, Chinese Critical Care Ultrasound Study, Findings of lung ultrasonography of novel corona virus pneumonia during the 2019-2020 epidemic, *Intensive Care Med.* 46 (5) (2020) 849–850.
- [89] S. Kulkarni, B. Down, S. Jha, Point-of-care (POC) lung ultrasound in intensive care during the COVID-19 pandemic, *Clin. Radiol.* 75 (9) (2020 May 13), 710.e.1–710.e.4.
- [90] D. Lichtenstein, I. Goldstein, E. Mourgeon, P. Cluzel, P. Grenier, J.J. Rouby, Comparative diagnostic performances of auscultation, chest radiography, and lung ultrasonography in acute respiratory distress syndrome, *J Am Soc Anesthesiologists* 100 (1) (2004 Jan 1) 9–15.
- [91] H. Sekiguchi, L.A. Schenck, R. Horie, et al., Critical care ultrasonography differentiates ARDS, pulmonary edema, and other causes in the early course of acute hypoxic respiratory failure, *Chest* 148 (4) (2015 Oct 1) 912–918.
- [92] G. Via, E. Storti, G. Gulati, L. Neri, F. Mojoli, A. Braschi, Lung ultrasound in the ICU: from diagnostic instrument to respiratory monitoring tool, *Minerva Anestesiol.* 78 (11) (2012 Nov 1) 1282–1296.
- [93] M.J. Smith, S.A. Hayward, S.M. Innes, A.S. Miller, Point of care lung ultrasound in patients with COVID-19—a narrative review, *Anaesthesia* 75 (8) (2020 Aug) 1096–1104.
- [94] ACR Guidance on COVID-19 and MR Use. [21](https://nam11.safelinks.protection.outlook.com/?url=https%3A%2Fwww.acr.org%2FClinical-Resources%2FRadiology-Safety%2FMR-Safety%2FCOVID-19-and-MR-Use&data=04%7C01%7CRevisedproof%40elsevier.com%7C61fc9952447940fcd7808d95f76c9dc%7C9274ee3f94254109a27f9fb15c10675d%7C0%7C0%7C637645787117575733%7CUnknown%7CTWFPbGZsb3d8eyJWJoiMC4wLjA wMDAiLjQlQjoiV2luMzliLjBtI16lk1haWwILCjXVCi6Mn0%3D%7C2000&data=mdf0w8SR7J53rdMqZVIR%2FHXOb3mQL3txhdk0aE51%2FvE%3D&reser ved=0. (Accessed October 2020).</p>
<p>[95] S. Kooraki, M. Hosseiny, S.S. Raman, L. Myers, A. Gholamrezaezhad, Coronavirus disease 2019 (COVID-19) precautions: what the MRI suite should know, <i>J. Am. Coll. Radiol.</i> 17 (7) (2020 Jul 1) 830.</p>
<p>[96] H. Syrjala, M. Broas, P. Ohtonen, A. Jartti, E. Pääkkö, Chest magnetic resonance imaging for pneumonia diagnosis in outpatients with lower respiratory tract infection, <i>Eur. Respir. J.</i> 49 (1) (2017 Jan 1).</p>
<p>[97] O.F. Ates, O. Taydas, H. Dheir, Thorax magnetic resonance imaging findings in patients with coronavirus disease (COVID-19), <i>Acad. Radiol.</i> 27 (10) (2020 Oct 1) 1373–1378.</p>
<p>[98] S. Yang, Y. Zhang, J. Shen, et al., Clinical potential of UTE-MRI for assessing COVID-19: patient and lesion based comparative analysis, <i>J. Magn. Reson. Imag.</i> 52 (2) (2020 Aug) 397–406.</p>
<p>[99] P. Torkian, H. Rajebi, T. Zamani, N. Ramezani, P. Kiani, S. Akhlaghpour, Magnetic resonance imaging features of coronavirus disease 2019 (COVID-19) pneumonia: the first preliminary case series, <i>Clin. Imag.</i> 69 (2021 Jan 1) 261–265.</p>
<p>[100] S. Maurea, C.G. Mainolfi, C. Bombace, et al., FDG-PET/CT imaging during the Covid-19 emergency: a southern Italian perspective, <i>Eur. J. Nucl. Med. Mol. Imag.</i> 47 (11) (2020 Oct) 2691–2697.</p>
<p>[101] S. Katal, H. Amini, A. Gholamrezaezhad, PET in the diagnostic management of infectious/inflammatory pulmonary pathologies: a revisit in the era of COVID-19, <i>Nucl. Med. Commun.</i> 42 (1) (2020 Dec 4) 3–8.</p>
<p>[102] M. Tulchinsky, J.S. Fotos, E. Slonimsky, Incidental CT findings suspicious for COVID-19-associated pneumonia on nuclear medicine examinations: recognition and management plan, <i>Clin. Nucl. Med.</i> 45 (7) (2020 Apr 9) 531–533.</p>
<p>[103] I. Alberts, B. Vollnberg, C. Sachpekidis, et al., Incidental SARS-CoV-2-related findings in asymptomatic patients in [18 F]-FDG-PET/CT—potential insights, <i>Eur. J. Nucl. Med. Mol. Imag.</i> 47 (2020 Aug) 2068–2069.</p>
<p>[104] C. Qin, F. Liu, T.C. Yen, X. Lan, 18 F-FDG PET/CT findings of COVID-19: a series of four highly suspected cases, <i>Eur. J. Nucl. Med. Mol. Imag.</i> (2020 Feb 22) 1–6.</p>
<p>[105] Y. Deng, L. Lei, Y. Chen, W. Zhang, The potential added value of FDG PET/CT for COVID-19 pneumonia, <i>Eur. J. Nucl. Med. Mol. Imag.</i> (2020 Mar 21) 1–2.</p>
<p>[106] S. Lütje, M. Marinova, D. Kitting, U. Attenberger, M. Essler, R.A. Bundschuh, Nuclear Medicine in SARS-CoV-2 pandemic: F-FDG-PET/CT to visualize COVID-19, <i>Nuklearmedizin</i> 59 (3) (2020 June) 276–280.</p>
<p>[107] F. Raffee, P. Keshavarz, S. Katal, et al., Coronavirus disease 2019 (COVID-19) in molecular imaging: a systematic review of incidental detection of SARS-CoV-2 pneumonia on PET studies, <i>Semin. Nucl. Med.</i> 51 (2) (2020 October) 178–191.</p>
<p>[108] M. Scarlattei, G. Baldari, M. Silva, et al., Unknown SARS-CoV-2 pneumonia detected by PET/CT in patients with cancer, <i>Tumori.</i> 106 (4) (2020 August) 325–332.</p>
<p>[109] S. Feng, W. Jun, S. Jun, et al., Review of Artificial Intelligence Techniques in Imaging Data Acquisition, Segmentation and Diagnosis for Covid-19, 2020 April. arXiv:2004.02731.</p>
<p>[110] J. Zhang, Y. Xie, Y. Li, C. Shen, Y. Xia, Covid-19 Screening on Chest X-Ray Images Using Deep Learning Based Anomaly Detection, 2020 March. arXiv:2003.12338.</p>
<p>[111] L. Wang, Z.Q. Lin, A. Wong, Covid-net: a tailored deep convolutional neural network design for detection of covid-19 cases from chest x-ray images, <i>Sci. Rep.</i> 10 (1) (2020 Nov 11) 1–2.</p>
<p>[112] J. Chen, L. Wu, J. Zhang, et al., Deep learning-based model for detecting 2019 novel coronavirus pneumonia on high-resolution computed tomography, <i>Sci. Rep.</i> 10 (1) (2020 Nov 5) 1–2.</p>
<p>[113] C. Zheng, X. Deng, Q. Fu, et al., Deep learning-based detection for COVID-19 from chest CT using weak label, <i>MedRxiv</i> (2020 Jan 1).</p>
<p>[114] S. Jin, B. Wang, H. Xu, et al., AI-assisted CT imaging analysis for COVID-19 screening: building and deploying a medical AI system in four weeks, <i>MedRxiv</i> 98 (2020 Jan 1).</p>
<p>[115] X. Xu, X. Jiang, C. Ma, et al., A deep learning system to screen novel coronavirus disease 2019 pneumonia, <i>Engineering</i> 6 (10) (2020 Oct 1) 1122–1129.</p>
<p>[116] L. Li, L. Qin, Z. Xu, et al., Artificial intelligence distinguishes COVID-19 from community acquired pneumonia on chest CT, <i>Radiology</i> 296 (2) (2020 Mar 19) E65–E71.</p>
<p>[117] F. Shi, L. Xia, F. Shan, et al., Large-scale Screening of Covid-19 from Community Acquired Pneumonia Using Infection Size-Aware Classification, 2020 March. arXiv:2003.09860.</p>
<p>[118] Z. Tang, W. Zhao, X. Xie, et al., Severity Assessment of Coronavirus Disease 2019 (COVID-19) Using Quantitative Features from Chest CT Images, 2020 March. arXiv:2003.11988.</p>
<p>[119] C. Jiehao, X. Jin, L. Daojiong, et al., A case series of children with 2019 novel coronavirus infection: clinical and epidemiological features, <i>Clin. Infect. Dis.</i> 71 (6) (2020 Sep 15) 1547–1551.</p>
<p>[120] W. Xia, J. Shao, Y. Guo, X. Peng, Z. Li, D. Hu, Clinical and CT features in pediatric patients with COVID-19 infection: different points from adults, <i>Pediatr. Pulmonol.</i> 55 (5) (2020 May) 1169–1174.</p>
<p>[121] X. Cui, T. Zhang, J. Zheng, et al., Children with coronavirus disease 2019: a review of demographic, clinical, laboratory, and imaging features in pediatric patients, <i>J. Med. Virol.</i> 92 (9) (2020 Sep) 1501–1510.</p>
<p>[122] Z. Wu, J.M. McGoogan, Characteristics of and important lessons from the coronavirus disease 2019 (COVID-19) outbreak in China: summary of a report of 72 314 cases from the Chinese Center for Disease Control and Prevention, <i>Jama</i> 323 (13) (2020 Apr 7) 1239–1242.</p>
<p>[123] Y.N. Duan, Y.Q. Zhu, L.L. Tang, J. Qin, CT features of novel coronavirus pneumonia (COVID-19) in children, <i>Eur. Radiol.</i> 30 (8) (2020 Aug) 4427–4433.</p>
<p>[124] T.H. Chang, J.L. Wu, L.Y. Chang, Clinical characteristics and diagnostic challenges of pediatric COVID-19: a systematic review and meta-analysis, <i>J. Formos. Med. Assoc.</i> 119 (5) (2020 May 1) 982–989.</p>
<p>[125] K. Feng, Y.X. Yun, X.F. Wang, et al., Analysis of CT features of 15 children with 2019 novel coronavirus infection, <i>Zhonghua er ke za zhi= Chin j pediatrics</i> 58 (2020 Feb 16) E007.</p>
<p>[126] H.J. Ma, J.B. Shao, Y.J. Wang, A.G. Zhai, N. Zheng, Q.J. Li, High resolution CT features of novel coronavirus pneumonia in children, <i>Chin. J. Radiol.</i> 54 (2020) 1005–1201.</p>
<p>[127] H.J. Li, S.Y. Liu, H.B. Xu, J.L. Cheng, Guideline for medical imaging in auxiliary diagnosis of coronavirus disease 2019, <i>Chin. J. Med. Imaging Technol.</i> 36 (3) (2020) 321–331.</p>
<p>[128] Y. Zhou, G.D. Yang, K. Feng, et al., Clinical features and chest CT findings of coronavirus disease 2019 in infants and young children, <i>Zhongguo Dang dai er ke za zhi= Chinese Journal of Contemporary Pediatrics</i> 22 (3) (2020 Mar 1) 215–220.</p>
<p>[129] A. Hasan, N. Mehmood, J. Fergie, Coronavirus disease (COVID-19) and pediatric patients: a review of epidemiology, symptomatology, laboratory and imaging results to guide the development of a management algorithm, <i>Cureus</i> 12 (3) (2020 Mar).</p>
<p>[130] F. Elshafeey, R. Magdi, N. Hindi, et al., A systematic scoping review of COVID-19 during pregnancy and childbirth, <i>Int. J. Gynecol. Obstet.</i> 150 (1) (2020 Jul) 47–52.</p>
<p>[131] Beregi JP, Greffier J. Low and Ultra-low Dose Radiation in CT: Opportunities and Limitations.</p>
<p>[132] M.A. Karimi, A. Radpour, A. Sedaghat, et al., Proposed imaging guidelines for pregnant women suspected of having COVID-19, <i>Acad. Radiol.</i> 27 (6) (2020 Jun 1) 902–903.</p>
<p>[133] N. Poyiadji, G. Shahin, D. Noujaim, M. Stone, S. Patel, B. Griffith, COVID-19-associated acute hemorrhagic necrotizing encephalopathy: imaging features, <i>Radiology</i> 296 (2) (2020 Aug) E119–E120.</p>
<p>[134] J. Helms, S. Kremer, H. Merdji, et al., Neurologic features in severe SARS-CoV-2 infection, <i>N. Engl. J. Med.</i> 382 (23) (2020 Jun 4) 226.</p>
</div>
<div data-bbox=)